DciA helicase operators exhibit diversity across bacterial phyla

Helen C. Blaine[1]*, Joseph T. Burke[2,3]*, Janani Ravi[2#], and Christina L. Stallings[1#]

[1]Department of Molecular Microbiology, Washington University School of Medicine, Saint Louis, Missouri 63110, USA.

[2]Departments of Pathobiology and Diagnostic Investigation, Microbiology and Molecular Genetics, Michigan State University, East Lansing, Michigan 48824, USA.

[3]Genomics and Molecular Genetics Undergraduate Program, Michigan State University, East Lansing, Michigan 48824, USA.

*Co-primary authors, contributed equally, listed alphabetically.

[#]Correspondence to stallings@wustl.edu and janani@msu.edu.

ABSTRACT

A fundamental requirement for life is the replication of an organism's DNA. Studies in *Escherichia coli* and *Bacillus subtilis* have set the paradigm for DNA replication in bacteria. During replication initiation in *E. coli* and *B. subtilis*, the replicative helicase is loaded onto the DNA at the origin of replication by an ATPase helicase loader. However, most bacteria do not encode homologs to the helicase loaders in *E. coli* and *B. subtilis*. Recent work has identified the DciA protein as a predicted helicase operator that may perform a function analogous to the helicase loaders in *E. coli* and *B. subtilis*. DciA proteins, which are defined by the presence of a DUF721 domain (termed the DciA domain herein), are conserved in most bacteria but have only been studied in mycobacteria and γ-proteobacteria (*Pseudomonas aeruginosa* and *Vibrio cholerae*). Sequences outside of the DciA domain in *Mycobacterium tuberculosis* DciA are

22 essential for protein function but are not conserved in the *P. aeruginosa* and *V. cholerae*
23 homologs, raising questions regarding the conservation and evolution of DciA proteins across
24 bacterial phyla. To comprehensively define the DciA protein family, we took a computational
25 evolutionary approach and analyzed domain architectures and sequence properties of DciA-
26 domain containing proteins across the tree of life. These analyses identified lineage-specific
27 domain architectures amongst DciA homologs as well as broadly conserved sequence-
28 structural motifs. The diversity of DciA proteins represents the evolution of helicase operation
29 in bacterial DNA replication and highlights the need for phylum-specific analyses of this
30 fundamental biological process.
31

32 IMPORTANCE

33 Despite the fundamental importance of DNA replication for life, this process remains
34 understudied in bacteria outside of *Escherichia coli* and *Bacillus subtilis*. In particular, most
35 bacteria do not encode the helicase loading proteins that are essential in *E. coli* and *B. subtilis*
36 for DNA replication. Instead, most bacteria encode a DciA homolog that likely constitutes the
37 predominant mechanism of helicase operation in bacteria. However, it is still unknown how
38 DciA structure and function compare across diverse phyla that encode DciA proteins. In this
39 study, we perform computational evolutionary analyses to uncover tremendous diversity
40 amongst DciA homologs. These studies provide a significant advance in our understanding of
41 an essential component of the bacterial DNA replication machinery.

42 # INTRODUCTION

43 DNA replication is a process critical to life for all organisms. The current paradigm for the
44 process of DNA replication in bacteria has primarily been based on studies in *Escherichia coli*
45 and *Bacillus subtilis*. Bacterial DNA replication begins with the binding of the replication
46 initiation protein DnaA to specific sequences referred to as DnaA boxes at the origin of
47 replication (oriC) (1–7). DnaA binding to double-stranded DNA (dsDNA) triggers DNA
48 unwinding at an AT-rich region of DNA called the DNA unwinding element (DUE), leaving a
49 bubble of single-stranded DNA (ssDNA) (1, 4, 6, 8, 9). The ssDNA bubble is coated by single-
50 stranded binding protein (SSB) (10), followed by the concerted loading of two hexameric
51 replicative helicases onto the SSB-coated replication fork. The two helicases translocate along
52 the two sides of the replication fork, unwinding the dsDNA as they move (1, 4, 5, 11–14).

53 Bacterial replicative helicases (DnaB in *E. coli* and DnaC in *B. subtilis*) are Superfamily IV
54 type helicases, which are defined as hexameric RecA ATPases (4, 15, 16) that translocate in the
55 5′-3′ direction (11, 12, 17) The bacterial replicative helicase translocates on ssDNA using a
56 "hand-over-hand" mechanism, which is driven by nucleotide hydrolysis (18, 19) (reviewed in
57 (17)). The C-terminus of the bacterial replicative helicase contains the RecA-like fold that is
58 responsible for the ATPase activity and is connected to an N-terminal scaffolding domain via a
59 linker region (1, 20, 21). The replicative helicase must oligomerize into a double-layered
60 hexameric ring to be active during replication, with one layer made up of the N-termini and the
61 other layer composed of the C-termini (1, 22, 23). In *E. coli* and *B. subtilis*, the loading of the
62 replicative helicase is performed with the help of a helicase loader, termed DnaC in *E. coli* and
63 DnaI in *B. subtilis* (4, 24–27). *dnaC* and *dnaI* were acquired by *E. coli* and *B. subtilis*, respectively,

64 via domestication of related but distinct phage ATPase-containing genes (28–31). DnaC and
65 DnaI are both in the ATPases Associated with diverse cellular Activities (AAA+) ATPase family,
66 and the ATPase activity of DnaC is required for its helicase loading function at the origin of
67 replication (32, 33).

68 *E. coli* and *B. subtilis* have long represented the paradigm of helicase loading during
69 bacterial replication. However, most bacteria do not encode ATPase helicase loader homologs
70 to DnaC or DnaI. Instead, most bacteria encode the ancestral protein, DciA (DnaC/I
71 Antecedent) (28, 34), which is defined by the presence of a Domain of Unknown Function
72 DUF721 (termed DciA domain herein). Despite the prevalence of DciA domain containing
73 proteins in bacteria (28), DciA homologs have only been studied in actinobacterial
74 (*Mycobacterium tuberculosis and Mycobacterium smegmatis)* and γ-proteobacterial
75 (*Pseudomonas aeruginosa* and *Vibrio cholerae*) species (28, 34–36). DciA homologs interact with
76 the replicative helicase DnaB and are essential for *M. tuberculosis*, *M. smegmatis*, and *P.*
77 *aeruginosa* DNA replication and viability (28, 34–36). Based on DciA's interaction with the
78 replicative helicase and requirement for DNA replication, DciA has been proposed to perform a
79 function analogous to that of the DnaC/I helicase loaders. However, DciA does not have a
80 predicted ATPase domain and, therefore, cannot be considered a helicase loader like DnaC/I.
81 Instead, DciA is referred to as a predicted helicase operator, although the mechanism of DciA
82 helicase operation is still unknown (28, 34).

83 Based on studies in *M. tuberculosis*, the DciA domain was predicted to contain a region
84 of structural homology to the N-terminus of DnaA (34), which was subsequently confirmed in
85 *V. cholerae* DciA (35, 36). The DciA domain in the *M. tuberculosis* DciA homolog is essential for

86 protein function (34). In addition, mycobacterial DciA homologs encode a 58 amino acid (aa)
87 sequence extension N-terminal to the DciA domain that is essential for *M. smegmatis* viability
88 (34). However, this sequence is not conserved in *P. aeruginosa* or *V. cholerae* DciA. Instead,
89 sequences C-terminal to the DciA domain in *V. cholerae* DciA that are not shared with
90 mycobacterial DciA are essential for the interaction between DciA and the replicative helicase
91 DnaB (35). Therefore, the DciA homologs in mycobacteria and the γ-proteobacteria *P.*
92 *aeruginosa* and *V. cholerae* have diverged in the relative position of the DciA domain and the
93 presence of N- or C-terminal sequence extensions. These sequence variations raise questions
94 of whether there are functional consequences of these differences and if a broader view of the
95 DciA protein family would reveal further diversification. To begin to address these open
96 questions, we took a computational evolutionary approach and analyzed the phylogenetic
97 distribution, domain architecture, and conservation of sequence properties amongst 26,789
98 DciA homologs. Our analysis revealed that most bacterial DciA proteins encode a single
99 annotated domain, the eponymous DciA domain. However, we also identified multiple DciA
100 homologs with novel domain architectures, which could provide clues to specialized functions
101 or biology in those bacteria. Amongst the bacterial DciA single-domain proteins, there was
102 lineage-specific variation in total protein length and positioning of the DciA domain. Despite
103 this variation in sequence properties, AlphaFold structural predictions (37) identified a broadly
104 conserved pattern of structural motifs where the DciA domain is connected to alpha-helical
105 structures via an unstructured linker. Therefore, our analyses reveal conserved sequence-
106 structural features of DciA homologs across bacterial phyla as well as lineage- and, sometimes,
107 species-specific features, highlighting the need for expanded studies of this protein family.

108 # RESULTS

109 ## DciA domain-containing proteins are predominantly found in bacteria with rare
110 transfers to eukaryota

111 A protein homology search with *M tuberculosis* DciA (AAK44227.1) only identifies closely
112 related homologs, predominantly in actinobacteria; similarly, homologs of *P. aeruginosa* DciA
113 (AAG07793.1) are mostly proteobacterial. These data suggest that the DciA homologs across
114 different phyla exhibit low conservation in their primary amino acid sequence. This divergence
115 warranted a more comprehensive approach that used multiple DciA-domain containing
116 proteins as starting points to retrieve the rich repertoire of DciA-like proteins from across the
117 tree of life. Therefore, we analyzed the ~27K InterPro entries for DciA domain-containing
118 proteins (DUF721; Dna[CI] antecedent DciA; Pfam ID entry PF05258) (38), excluding
119 metagenome data entries. We also added valuable metadata to this dataset, including protein
120 accession numbers, taxID, species, and complete and collapsed lineages for each protein
121 **(Table S1,** https://github.com/JRaviLab/dcia_evolution). Our initial characterization revealed
122 that these ~27K DciA-like proteins spanned the three kingdoms of life with 37 bacterial (with
123 assigned lineages), 76 bacterial candidatus lineages (yet unassigned), 5 archaeal, 1 viral, and 6
124 eukaryotic lineages.

125 Next, we analyzed the phyletic distribution and domain architectures of all ~27K DciA
126 proteins using the MolEvolvR web application (39). This analysis highlighted that most (99.9%)
127 proteins were found in the kingdom eubacteria **(Fig. 1A).** In addition, there were 26 DciA

128 domain-containing proteins from eukaryota, archaea, and viral sequences **(Fig. 1A and Table**
129 **S2)**. We performed BlastP homology searches with the 26 non-bacterial DciA domain-
130 containing proteins (40) and found that over 95% of top hits with the highest confidence levels
131 retrieved for 24 of these proteins were from bacterial genomes, suggesting that these DciA-
132 domain containing proteins had been mistakenly attributed to archaeal, eukaryotic, or viral
133 genomes **(Table S2)**. The two remaining non-bacterial DciA-like proteins occur in *Kingdonia*
134 *uniflora* (KAF6150485.1), an endangered angiosperm with over-representation in DNA
135 replication and repair genes (41), and the fungus *Hyaloscypha bicolor E* (PMD57303.1) **(Table S2,**
136 **Fig. S1A)**. All close homologs of the *K. uniflora* DciA protein were in magnoliopsida, a class of
137 flowering plants. The DciA protein from *H. bicolor E* predominantly retrieved (98/100) DciA-like
138 proteins in fungal species. We also verified that these two eukaryotic DciA proteins were part
139 of annotated ORFs in complete genomes, suggesting that they are truly eukaryotic proteins.
140 Further, using AlphaFold structure prediction, we found that the DciA domains within the *K.*
141 *uniflora* and *H. bicolor E* proteins resembled a truncated version of the *V. cholerae* DciA domain,
142 solved previously using NMR (36) **(Fig. S1B)**. Each eukaryotic DciA domain is approximately
143 half of the median length of *V. cholerae* DciA domain and is predicted to contain just the first
144 alpha-helix and beta-sheet present in the *V. cholerae* DciA domain **(Fig. S1B)** (36). Our analysis
145 using MolEvolvR revealed that the DciA domain-containing protein in *K. uniflora* also carries an
146 annotated HMA (heavy metal associated) domain (Pfam: PF00403), overlapping with the DciA
147 domain **(Fig. S1A,B)**. HMA domains are typically involved in heavy metal transport and
148 detoxification in both eukaryotic and prokaryotic species (42–44), where heavy metal exposure
149 can induce DNA damage (45–47). Although there were no additional Pfam domains annotated

150 in the *H. bicolor E* DciA domain-containing protein, we identified two AN11006-like domains
151 (PANTHER family: PTHR42085) of unknown function on either side of the DciA domain **(Table**
152 **S2)**. Given that the DciA domain was previously considered to be an exclusively bacterial
153 protein domain, the identification of predicted DciA structural domains in two eukaryotic
154 species reveals the potential for much broader evolutionary distribution than previously
155 appreciated, providing avenues for future structure-function studies.

156 Bacterial DciA homolog domain architectures

157 *DciA domains are mostly loners*

158 The bacterial DciA proteins from InterPro fell into 37 bacterial lineages **(Fig. 1A)**, plus many
159 sequences annotated as Candidatus due to incomplete taxonomic classification **(Table S1,**
160 https://github.com/JRaviLab/dcia_evolution). In line with sequencing and publication bias,
161 proteobacterial, actinobacterial, and bacteroidetes genomes were over-represented in our
162 homolog space (48–50) **(Fig. 1A)**. Given the variation noted in the two eukaryotic DciA-domain
163 containing proteins, we then proceeded to characterize the domain architecture of the ~26K
164 bacterial DciA homologs using MolEvolvR (39). We found that a stark majority (99.7%) of
165 bacterial DciA proteins carried a lone DciA domain. In addition, we identified 38 variations
166 where DciA homologs either contained multiple DciA domains or additional annotated
167 domains **(Fig. 1B,C).** The domain architecture variations were often lineage-specific, as
168 described below, indicating that they evolved later during speciation to adapt to lineage-
169 specific biology.

170 *Proteobacterial-specific variations in DciA domain architecture*

171 Within proteobacteria, we identified four lineage-specific DciA domain architectures **(Fig. 1B)**,
172 including some domains present in other proteins associated with DNA replication**.**
173 Specifically, 15 proteobacterial DciA homologs contained a thioredoxin-like domain (Pfam:
174 Thioredoxin (TRX) PF13462; *e.g.,* ODT99650.1, *Rhodospirillales*) **(Fig. 1B,C)**. TRX domains are
175 present in a large class of redox-regulated proteins (51), and play roles in oxidative stress
176 responses (52, 53). In addition, *Cc*TRX1, an essential TRX domain protein, is upregulated during
177 DNA replication initiation in the α-proteobacteria *Caulobacter crescentus* (54). Two other
178 proteobacterial DciA homologs contain PDZ domains (Pfam: PF13180; e.g., KQZ00574.1,
179 *Pseudolabrys*) **(Fig. 1B,C)**, which are generally involved in protein-protein interactions (55, 56)
180 and could facilitate the interaction between these DciA proteins and other replication proteins.
181 The PDZ domain-containing DciA homologs also carry trypsin-like peptidase domains (Pfam:
182 PF13365) **(Fig. 1B,C)**, which have recently been linked to DNA replication in humans, where the
183 trypsin-like peptidase domain in the protein FAM111A is necessary for overcoming replication
184 fork stalling (57). The DciA homolog in the α-proteobacteria *Micavibrio aeruginosavorus*
185 (PZQ43964.1) encodes three translation elongation factor P domains (KOW-like, Pfam:
186 PF0820, OB, Pfam: PF01132, C-terminal, Pfam: PF09285) **(Fig. 1B,C)**.

187 *Actinobacterial variations in DciA domain architectures*

188 We identified four distinct lineage-specific domain architectures within actinobacteria, all of
189 which involve domains associated with nucleotide sensing and DNA replication. Three
190 Streptomyces DciA homologs contain a YspA domain (Pfam: YAcAr/PF10686; *e.g.,*

191 SNC77843.1) in addition to the DciA domain **(Fig. 1B,C)**. YspA domains typically have fusions
192 to domains that sense and process nucleotide-derived ligands such as ADP-ribose (58). We
193 found that the DciA protein in *Bifidobacterium callitrichos* (PST49340.1) contains the C-terminal
194 domain of the DEAD-box RNA helicase family (Pfam: PF00271) (59), and the res subunit of the
195 type III restriction enzyme, which encodes ATPase activity (Pfam: PF04851) (60) **(Fig. 1B,C)**. In
196 addition, five actinobacterial DciA homologs contain an N-terminal RecF/RecN/SMC domain
197 (Pfam: 02463; *e.g.*, OUE04448.1, *Clavibacter*) **(Fig. 1B,C)** common in the N-termini of structural
198 maintenance of chromosome (SMC) proteins. The SMC domain typically includes an NTP-
199 binding motif and SMC proteins are involved in chromosome partitioning, DNA recombination,
200 and repair (61–65). In addition, six actinobacterial DciA homologs contain multiple DciA
201 domains (e.g. OEJ23183.1, *Streptomyces*) **(Fig. 1B,C)**.

202 In addition to actinobacteria-specific domain architectures, DciA proteins in
203 *Micromonospora endolithica* (RKN42798.1) and bacteroidetes species *Rhodothermus marinus*
204 (BBM73918.1, ACY49481.1) contain the γ/τ (Pfam: PF12169) and δ(Pfam: PF13177) subunit
205 domains of DNA polymerase III **(Fig. 1B,C)**, which make up part of the clamp loader complex in
206 *E. coli* (66, 67). The DNA pol III domains present in these DciA homologs also contain AAA+
207 ATPase domains, also found in DnaC/DnaI helicase loaders from *E. coli* and *B. subtilis* (29, 32,
208 33, 67).

209 *Other DciA domain architectures involving domains associated with DNA replication*

210 Thirty-six DciA homologs from nitrospinae and candidatus rokubacteria were annotated to
211 contain tetratricopeptide repeat (TPR) domains **(Fig. 1B,C)**. TPR domains are largely

212 eukaryotic protein-protein interaction domains (68). For example, the TPR domain of the
213 replication regulator Dia2 in eukaryotes is essential for the association of Dia2 with the
214 replisome progression complex, which interacts with the MCM2-7 helicase at the replication
215 fork (69). TPR proteins have also been identified in bacteria. For example, in the α-
216 proteobacteria *Orientia tsutsugamushi*, two TPR proteins bind to the eukaryotic RNA helicase
217 DDX3 to inhibit host cell translation (70). In candidatus rokubacteria, these TPR repeats are
218 sometimes associated with an anaphase-promoting complex domain (Pfam: PF12895; *e.g.*,
219 OLB41025.1), which along with TPR repeat domains, is present in eukaryotic cell cycle
220 regulators (71, 72).

221 The DciA homologs from two planctomycetes (KAF0244841.1, NUN49423.1) contain a
222 Histidine kinase-, DNA gyrase B-, and HSP90-like ATPase domain (Pfam: PF02518), a DNA
223 gyrase B domain (Pfam: PF00204), a toprim domain (DNA topoisomerase II Pfam: PF01751),
224 and a DNA gyrase B C-terminus domain (Pfam: PF00986). A closer look at one of the
225 planctomycetes DciA sequences (KAF0244841.1) shows that DciA and GyrB are annotated as a
226 single fused protein. GyrB, part of the bacterial gyrase, is responsible for the negative
227 supercoiling of dsDNA, which is essential during the opening of the DNA replication bubble
228 (73).

229 *Homology search with multiple starting points identifies additional DciA domain*
230 *architectures*

231 To ensure that we identified all sequenced DciA homologs and the entire repertoire of domain
232 architectures in this protein family, we selected 94 unique lineage-domain-architecture pairs

233 from 36 bacterial lineages and 27 total domain architectures to identify novel DciA homologs
234 across the tree of life using MolEvolvR **(Fig. S2A)**. The only phylum without a representative
235 from our initial analysis was atribacterota, which did not contain class-level assignments. In
236 addition to novel domain architectures discussed above, the homology search identified 8 new
237 domain architectures, including 11 actinobacterial homologs with a DciA dyad (*e.g.*,
238 WP_165395910.1 from *Streptomyces*), several fusions with TPR repeats, and a DciA domain
239 fused with an aminomethyltransferase domain (*Micrococcus sp. HSID17227*, WP_238693333.1)
240 **(Fig. S2B)**. Together, our initial characterization along with these homologs captured the rich
241 repertoire of DciA variation.

242 DciA single-domain homologs vary in protein length and position of the DciA 243 domain

244 Despite having only one annotated domain, the DciA single-domain proteins varied
245 considerably in length, ranging from 32 to 482 amino acids **(Fig. 2A)**. In addition to total
246 protein length, the distance of the DciA domain from the N- or C-terminus varied widely,
247 where the DciA domain sometimes fell in the middle, at the N-terminus, or at the C-terminus
248 of the protein **(Fig. 2A)**. The median amino acid length of the annotated DciA domains in our
249 dataset is 85aa **(Table S1)**, indicating that DciA homologs close to this protein length would
250 only contain the DciA structural domain. An example of a DciA protein where the total protein
251 length is similar to the size of the single DciA structural domain is the *Bacteroides fragilis* DciA
252 homolog (AUI45441.1), which is 96aa long with the DciA domain annotated from amino acids
253 8-95. The AlphaFold structural prediction tool predicts that the entire *B. fragilis* DciA protein is

254 comprised of the predicted DciA domain structure, consisting of one alpha-helix followed by a
255 two beta-sheet motif, one kinked alpha-helix, and a third beta-sheet (34, 36) **(Fig. 2B)**.
256 However, with a median protein length of 148aa **(Fig. 2A),** most DciA single-domain proteins
257 are longer than the typical DciA domain length, suggesting that there may exist other
258 functional sequences in DciA single-domain proteins that are not annotated as domains. For
259 example, *V. cholerae* DciA is 157aa long, with the DciA domain positioned at the N-terminus
260 (amino acids 12–90) followed by a 67aa C-terminal sequence extension. An NMR structure of
261 the N-terminus of *V. cholerae* DciA confirms that the DciA domain in the N-terminus is
262 sufficient to form the DciA domain structure (36). In addition to confirming the DciA domain
263 structure in the N-terminus, AlphaFold prediction of the full-length *V. cholerae* DciA protein
264 (AAF95538.1) depicts the C-terminus as an alpha-helix immediately following the DciA domain,
265 connected to two terminal alpha-helices by an 11aa linker **(Fig. 2B)**. Given that the C-terminus
266 of *V. cholerae* DciA is required for its interaction with the replicative helicase *in vitro* (35), these
267 data demonstrate not only that most DciA single-domain homologs are longer than the DciA
268 domain alone, but also that the sequence extensions appended to the DciA domain can be
269 physiologically relevant. The identification of DciA homologs with different domain
270 architectures **(Fig. 1)**, varying protein lengths **(Fig. 2A)**, and different positioning of the DciA
271 domain **(Fig. 2A)** suggest that some DciA homologs have evolved sequence properties with
272 likely functional consequences for DciA activity.

273 Many DciA single-domain homologs are predicted to encode intrinsically
274 disordered regions

275 Small-angle X-ray scattering, intrinsic disorder prediction tools, and molecular dynamic
276 simulations have shown that the C-terminus of *V. cholerae* DciA that is required for DnaB
277 binding *in vitro* contains an IDR (35). In addition, there is precedent for IDRs in other bacterial
278 DNA replication proteins, including SSB (74–77), the replication restart helicase Rep (78, 79),
279 the helicase loaders DnaC and DnaI, and the replication initiation protein DnaA (35). To
280 estimate the co-occurrence of IDRs with DciA domains, we used MobiDBLite (from within
281 MolEvolvR (80)) to predict IDRs in each of the bacterial DciA homologs **(Table S1; Fig. 3A)**. Out
282 of ~23K total bacterial non-candidatus DciA single-domain homologs, ~8K proteins contained
283 at least one IDR, and some (4,728) had multiple regions of disorder predicted. These IDRs were
284 present in DciA homologs from 24 phyla **(Fig. 3A)**. Analysis of the lengths of the IDRs in the
285 DciA homologs from each phyla found that these IDRs ranged in length from 14aa to 213aa
286 **(Fig. 3B)**. *M. tuberculosis* DciA was among the single-domain proteins predicted to contain
287 IDRs both N- and C-terminal to the DciA domain. Deletion of the N-terminal sequence of *M.*
288 *tuberculosis* DciA that encodes the predicted IDR renders mycobacteria nonviable,
289 demonstrating that this region predicted to form an IDR in DciA is essential for its cellular
290 function (34).

291 DciA single-domain homologs can be separated into four groups based on
292 protein length and the positioning of the DciA domain

293 The importance of the predicted IDR sequences for DciA activity in *M. tuberculosis* (34) and *V.*
294 *cholerae* (35) along with the prevalence of predicted IDRs in DciA homologs suggest that IDRs
295 in other DciA homologs may also be functionally relevant. In addition, we hypothesized that
296 the N- and C-terminal sequence extensions in DciA single-domain proteins without predicted
297 IDRs may also be functionally relevant. Since the minimum IDR sequence length in DciA
298 homologs was 14aa **(Fig. 3B)**, we reasoned that any N- or C-terminal sequence extension
299 ≥14aa in a DciA protein could comprise a functionally relevant sequence. To identify DciA
300 proteins with potentially relevant sequence extensions associated with the DciA domain, we
301 binned the bacterial non-candidatus DciA single-domain homologs (23,309 total proteins) into
302 four groups: i) Group 1 proteins with ≥14aa N-terminal to the DciA domain and <14aa C-
303 terminal, ii) Group 2 proteins with <14aa N-terminal to the DciA domain and ≥14aa C-terminal,
304 iii) Group 3 proteins with ≥14aa both N- and C-terminally to the DciA domain, and iv) Group 4
305 proteins with <14aa on both N- and C-termini **(Fig. 4 top panel, Table S1)**.

306 Most (~90%) actinobacterial DciA homologs fell into Group 3, with sequences on both
307 sides of the DciA domain, although there were examples of actinobacterial DciA proteins in
308 each of the other three groups as well **(Fig. 4A)**. When we separated actinobacteria by class,
309 we found that actinomycetia and coriobacteria DciA proteins were mostly in Group 3, whereas
310 acidimicrobia, nitriliruptoria, and thermoleophilia DciA proteins were mostly in Group 1 **(Fig.**
311 **4B)**. Group 3 also contained several (~65%) proteobacterial DciA homologs, however, there
312 were also 2,958 proteobacterial DciA proteins in Group 2, as well as representatives in Groups 1

313 and 4 **(Fig. 4A)**. When we separated proteobacteria into individual classes, homologs from α-
314 proteobacteria, β-proteobacteria, δ-proteobacteria, γ-proteobacteria, oligoflexia, and ζ-
315 proteobacteria fell mostly into Group 3 **(Fig. 4B).** In contrast, DciA homologs in ε-
316 proteobacteria and hydrogenophila mostly fell into Group 2. In contrast to both actinobacteria
317 and proteobacteria, bacteroidetes DciA homologs fell almost exclusively into Groups 1 and 4,
318 with the majority (~84%) belonging to Group 4 **(Fig. 4A)**. When we separated bacteroidetes
319 into classes, we found that only the cytophagia bacteria contained mostly Group 1 homologs,
320 while the rest of bacteroidetes classes contained mostly Group 4 homologs, indicating lineage
321 and class-specific selection of DciA homolog sequence structures **(Fig. 4B).**

322 To better visualize the distribution of DciA single-domain proteins from phyla with
323 smaller numbers of representative sequences, we removed the proteobacterial,
324 actinobacterial, or bacteroidetes sequences and plotted the distribution of the remaining DciA
325 single-domain homologs in Groups 1–4 **(Fig. 4C)**. Some lineages had almost all DciA homologs
326 classed within a single Group, indicating the evolution and conservation of a particular DciA
327 sequence organization for that lineage. For example, 94% of verrucomicrobia and 96% of
328 chlamydiae DciA homologs fell into Group 1. Other lineages had DciA homologs more broadly
329 distributed across Groups, although there were still lineage-specific biases towards single
330 Groups. Greater than 65% elusimicrobia, lentisphaerae, ignavibacteriae, and fibrobacteres
331 DciA proteins were classed into Group 1, >65% of cyanobacteria, nitrospirae, deinococcus-
332 thermus, and thermodesulfovibrio DciA homologs were classed in Group 2, and >65% of
333 synergistetes DciA homologs are in Group 3. Planctomycetes exhibited differentiation of DciA
334 homolog grouping at the Class level. Planctomycetes class planctomycetia homologs were

335 mostly in Group 1, while planctomycetes phycisphaerae homologs were split evenly between
336 Groups 1 and 3 (**Fig. 4C, Table S1**). Firmicute and fusobacteria DciA homologs were
337 represented equally in Groups 2 and 3, with a small number of representatives in groups 1 and
338 4. Alternatively, gemmatimonadetes DciA homologs were predominantly split between
339 Groups 1 and 4, and nitrospinae homologs were split between groups 1 and 2.

340 In addition to bacteroidetes, other lineages that were predominantly in Group 4
341 included chloroflexi (56% of DciA homologs), rhodothermaeota (81%), calditrichaeota (74%),
342 chlorobi (86%), and thermotogae (91%) **(Fig. 4C)**. Group 4 proteins only encode the DciA
343 structural domain, indicating that the DciA domain is sufficient for DciA activity in these
344 bacteria, although this has yet to be experimentally tested. DciA homologs from acidobacteria,
345 spirochaetes, and armatimonadetes did not follow any apparent trends in DciA homolog
346 classification, and kiritimatiellaeota, aquificae, chrysiogenetes, abditibacteriota, tenericutes,
347 balneolaeota, caldiserica, dictyoglomi, atribacterota, and deferribacteres had <20 sequences in
348 our dataset. The lineage and class-specific trends observed in the four different DciA groupings
349 suggest differentiation of DciA proteins in a largely lineage-specific manner. The sequences N-
350 and/or C-terminal to the DciA domain in Groups 1–4 could have functional consequences for
351 the mechanisms of DciA proteins in different bacterial lineages.

352 Structure predictions of DciA single-domain homologs reveal conserved 353 structural motifs within and outside of the DciA domain

354 To understand the impact of sequence extensions on protein structure in DciA single-domain
355 homologs, we used AlphaFold structure prediction to model representative DciA proteins from

356 Groups 1–4 **(Fig. 5)**. For Groups 1–3, we also compared the structures of homologs with and
357 without IDRs predicted in the sequence extensions. Regardless of Group designation, all DciA
358 domains were predicted to fold into a structure similar to that previously predicted for *M.*
359 *tuberculosis* DciA (34) and experimentally validated for *V. cholerae* DciA (36) **(Fig. 5)**.

360 For a Group 1 DciA from planctomycetes (KLU02380.1, *Rhodopirellula islandica*) that is
361 predicted to have a 48aa IDR N-terminal to the DciA domain, AlphaFold predicts that the N-
362 terminal sequence extension does not form any structured helices or beta sheets, supporting
363 that this region could be intrinsically disordered **(Fig. 5)**. In contrast, the structural prediction of
364 a Group 1 DciA single-domain protein from bacteroidetes (GEO04242.1, *Adhaeribacter*
365 *aerolatus*) with no predicted IDR displays the C-terminal sequence extension ending with a
366 single alpha-helix, connected to the DciA protein with an unstructured linker **(Fig. 5)**.

367 A Group 2 DciA homolog from cyanobacteria (AFY85399.1, *Oscillatoria acuminata*) that
368 is predicted to contain a C-terminal IDR exhibited the classic DciA domain folds followed by
369 one alpha helix connected to two more C-terminal helices via a 24aa linker, which coincided
370 with the predicted IDR **(Fig. 5)**. The Group 2 DciA homolog from *P. aeruginosa* (AAG07793.1, γ-
371 proteobacteria) with no predicted IDR, contains the DciA domain folds connected to two C-
372 terminal helices via a 16aa linker **(Fig. 5)**, which is reminiscent of the structure for O. *acuminata*
373 DciA, .

374 The Group 3 DciA protein from the actinobacteria *M. tuberculosis* (BAL63824.1) consists
375 of a single 18aa alpha helix in its N-terminus that is connected to the DciA domain by a 34aa
376 linker region, which is predicted to contain an IDR **(Fig. 5)**. The C-terminus of *M. tuberculosis*
377 DciA is also predicted to contain a 19aa IDR. A group 3 protein with no predicted IDR from

378 *Leptospira interrogans* (spirochaete (AAN47203.1) contains sequence extensions in both its N-
379 and C-terminus **(Fig. 5)**, with the same double alpha helix fold in its C-terminus as observed in
380 the group 2 proteins *P. aeruginosa* and *O. acuminata.* The DciA domain is also connected to the
381 two-alpha helical domain by a 20aa unstructured linker region.

382 Similar to the structure predicted for *B. fragilis* DciA **(Fig. 2B),** other Group 4 DciA
383 homologs from thermotogae (*Thermotoga maritima*, AAD35914.1) and α-proteobacteria
384 (*Rickettsia conorii*, AAL03818.1) only contain the folds previously reported for the DciA domain
385 in *V. cholerae* (36) **(Fig. 5)**. These data further support that the DciA structural domain alone is
386 sufficient for DciA activity in Group 4 bacteria.

387 Visualization of these representative DciA structures reveals that when unannotated
388 sequences are appended to the DciA domain (Groups 1–3), they tend to form an unstructured
389 linker region connected to 1–2 alpha-helices at the termini, regardless of whether the
390 sequences are positioned N- or C-terminal to the DciA domain. In some Group 1–3 DciA
391 homologs, the linker is predicted to comprise an IDR. Notably, *V. cholerae* DciA has an
392 experimentally verified C-terminal IDR (35), although this was not predicted by MobiDBLite
393 **(Table S1)**. Circular dichroism and secondary structure prediction tools of *V. cholerae* DciA
394 predict that the C-terminal IDR can transiently form two alpha-helices (35) **(Fig. 2B)**. These
395 helices occur at a similar position in *P. aeruginosa* DciA as well **(Fig. 5)**. Therefore, it is possible
396 that the unstructured linker motifs in *P. aeruginosa* and other Group 1–3 DciA homologs
397 comprise IDRs not predicted by MobiDBLite due to the alpha-helices that can form in the
398 termini. The conservation of the predicted structures of DciA homologs across bacterial
399 lineages, where the DciA domain is connected to alpha-helical structures via an unstructured

400 linker, suggests that these structural motifs are important for DciA activity in bacteria that
401 encode Group 1–3 homologs.

402 DciA evolution across the tree of life

403 Our sequence-structure analyses thus far revealed lineage-specific signatures in DciA domain
404 organization in addition to the widely prevalent DciA single-domain proteins. The natural next,
405 and final, question is how did these different DciA proteins evolve — are there species/lineage-
406 specific, domain architecture, or group-specific migration patterns? To address these
407 questions, we used all DciA proteins from **Fig. 1** to generate a phylogenetic tree **(Fig. 6)**. Most
408 strikingly, we observed that DciA homologs clustered by lineages **(Fig. 6A).** The three largest
409 lineages, actinobacteria, bacteroidetes, and proteobacteria, are labeled based on their
410 dominant membership **(Fig. 6A)**. We noted two main proteobacterial clades (left and bottom),
411 likely due to class-wise grouping. We, therefore, further resolved the tree by the predominant
412 bacterial classes from these three phyla **(Fig. 6B)**. The class-resolved tree explains the distinct
413 proteobacterial clusters observed in the phylum-based tree **(Fig. 6A),** wherein α-
414 proteobacteria and β/γ-proteobacteria form distinct clusters **(Fig. 6B)**. This migration pattern
415 of the α-proteobacterial homologs suggests that the DciA proteins in this lineage have
416 diverged evolutionarily from the rest of the proteobacterial lineages. The phylogenetic analysis
417 indicates that variations in DciA protein domain architectures, protein lengths, and DciA
418 domain positioning likely occurred after lineage-specific divergence of bacterial classes.
419 Overall, the DciA phylogenetic tree delineates the evolution of this critical panbacterial protein
420 across all major lineages.

421

422 # DISCUSSION

423 The recent discovery of DciA as a predicted helicase operator in bacteria (28, 34, 36) has begun
424 to shed light on a long-standing open question of how the majority of bacteria facilitate
425 helicase activity during DNA replication in the absence of the ATPase helicase loaders
426 expressed by *E. coli* and *B. subtilis*. The wide distribution of DciA in diverse bacterial phyla
427 indicates that these proteins likely represent the predominant paradigm for helicase operation,
428 despite not being conserved in *E. coli* and *B. subtilis,* the organisms typically used as a model
429 for bacterial replication. DciA proteins are defined by the presence of the DciA domain (28).
430 Prior phylogenetic analysis indicates that *dnaC* and *dnaI* homologs were acquired through
431 evolution at the expense of *dciA* (named for *dna[CI]* antecedent) (28, 30, 31) suggesting that
432 DciA and DnaC/DnaI perform a common function. In addition, it has been shown that DciA
433 interacts with the replicative helicase and is required for DNA replication and viability in the
434 few organisms it has been studied in (28, 34–36). However, the mechanism by which DciA
435 mediates replication initiation is still unknown.

436 Our comprehensive evolutionary study of DciA proteins has revealed both lineage-
437 specific and conserved features amongst homologs. We find that most homologs are DciA
438 single-domain proteins in bacteria, with rare instances of additional domains in DciA
439 homologs, many of which have known roles in DNA replication and repair **(Fig. 1, S2)**. These
440 additional domain architectures were predominantly phyla-, and sometimes species-, specific,
441 suggesting that they have been acquired and maintained to facilitate lineage-specific

442 requirements during DNA replication. Further study of these DciA domain architectures could
443 shed light on varying mechanisms of the regulation of bacterial replication, or other roles for
444 DciA in the cell. Similarly, we identified two eukaryotic proteins that encode partial DciA
445 domains **(Fig. S1)**, raising the question of how this domain would function in eukaryotes in the
446 absence of its bacterial replicative helicase binding partner. The eukaryotic DciA-domain
447 containing proteins also harbored additional domains without known connections to DNA
448 replication, possibly suggesting that the DciA domain has been co-opted for other purposes in
449 these organisms.

450 Even though most bacterial DciA homologs were single-domain proteins, they
451 exhibited a wide variety in sequence lengths and positioning of the DciA domain **(Fig 2, Table**
452 **S1)**. When we grouped the DciA homologs based on the position of the DciA domain and the
453 presence of N- and C-terminal extensions, we identified lineage-specific trends in these
454 sequence features **(Fig. 4)**, suggesting that these variations mostly evolved following
455 speciation and highlight how the regulation of helicase activity during DNA replication
456 initiation could differ between phyla. For example, most actinobacterial and proteobacterial
457 DciA single-domain homologs fell into Groups 2 and 3, which harbored sequence extensions
458 either N-terminally or on both sides of the DciA domain, while most bacteroidetes DciA
459 homologs were classed in Group 4 encoding only the DciA structural domain. The sequence
460 extensions in actinobacteria *M. tuberculosis* and proteobacteria *V. cholerae* DciA have been
461 shown to be essential for DciA activity *in vivo* or *in vitro*, respectively (34, 35). The absence of
462 these sequences in most bacteroidetes homologs suggests differing requirements for DciA
463 activity in different bacteria.

464 Despite the lineage-specific grouping of DciA homologs based on sequence lengths and
465 positioning of the DciA domain, AlphaFold structural prediction of representative DciA
466 homologs from each Group revealed common structural patterns **(Fig. 5)**. The DciA domain
467 structure (36) was conserved across DciA homologs, and has previously been noted to
468 resemble the structure of the N-terminus of DnaA (34–36, 81). The N-terminus of DnaA is
469 critical for the interaction with the DnaB replicative helicase and other regulators (82, 83),
470 however, the role of the DciA domain in the interaction with DnaB has yet to be established. A
471 tryptophan residue conserved in the DciA domains of many DciA homologs is positioned
472 similarly to a phenylalanine residue in the DnaA N-terminus that has been predicted to have a
473 key role in making contacts between DnaA and its interacting partners, including DnaB (34,
474 84). Mutation of the tryptophan in the DciA domain of *M. tuberculosis* DciA results in slow
475 growth and decreased DNA replication (34). This supports that the tryptophan within the DciA
476 domain plays a key role for DciA function *in vivo* in mycobacteria. However, not all DciA
477 homologs encode this tryptophan residue within their DciA domain, a key example being *V.*
478 *cholerae* DciA, which has an isoleucine at this position (35). Therefore, even the defining DciA
479 domain feature of DciA proteins exhibits some variation in different bacteria that may reflect
480 differences in mechanism of action or mode of interaction with the replicative helicase.

481 In addition to conservation of the DciA domain structure, when sequence extensions
482 were associated with the DciA domain, they tended to form unstructured linkers terminating in
483 1–2 alpha-helices **(Fig. 5)**. These linker and alpha-helical structures were identified either C- or
484 N-terminal to the DciA domain, depending on the homolog, where the role of this positioning
485 in terms of function is still unknown. At least one third of the DciA single-domain homologs

486 were also predicted to contain IDRs **(Fig. 3, 5)**. The IDR C-terminal to the DciA domain in the *V.*
487 *cholerae* homolog is required for its interaction with the DnaB helicase (35). IDRs in other
488 replication proteins, including SSB and Rep, also play key roles in facilitating protein-protein
489 interactions within the replisome (74–79), indicating a common theme and function of these
490 domains during bacterial DNA replication. However, if the IDR in the unstructured linker
491 sequence is required for the interaction between DciA and the replicative helicase, this would
492 imply that Group 4 DciA homologs, which only encode the DciA structural domain and no
493 linker domains, employ other sequences or mechanisms to interact with DnaB. Thus far, no
494 DciA homologs in Group 4 have been studied either genetically or biochemically and so how
495 the DciA domain functions on its own remains a mystery.

496 Our computational evolutionary analyses have enabled an in-depth delineation of the
497 evolution of DciA across the tree of life and elucidated the variation in DciA domain
498 architectures, co-occurrences with IDRs, and the many flavors of bacterial DciA sequence-
499 structural features. Despite this deep exploration, many unknowns still remain regarding DciA
500 proteins and bacterial DNA replication. Our results highlight the complexities and diversity
501 that have evolved in the fundamental process of DNA replication, where no single species of
502 bacteria will be able to represent a central dogma that holds true throughout the kingdom.
503 These studies provide a framework for researchers to consider the evolutionary variation while
504 dissecting the mechanistic basis for helicase operation in bacteria.

505

506 # METHODS

507 ## Query selection

508 We started with ~27K DciA carrying proteins from Pfam (UniProt sequences from the InterPro
509 database (38)). We added relevant metadata to each of these homologs, including
510 corresponding NCBI protein accession numbers, protein length, taxID, species, and lineages.
511 We used MolEvolvR (39) and the underlying InterProScan (85) to explore the domain
512 architectures, cellular localizations, and disorder predictions for all ~27K DciA proteins. The
513 resulting domain architectures (from MolEvolvR) were also appended to each homolog's
514 metadata. All these data are available in **Table S1**, and on GitHub
515 (https://github.com/JRaviLab/dcia_evolution).

516

517 *Representative DciA proteins*: To select representatives for subsequent analyses, we picked
518 DciA carrying proteins from each lineage–domain-architecture combination. We excluded
519 proteins that were not bacterial, and those without an assigned lineage, (*e.g.*, candidatus and
520 uncultured bacteria). The remaining sequences were then grouped by the short lineage column
521 (superkingdom>phylum>class) and the Pfam domain architecture column. These groups were
522 then reverse sorted by sequence completeness and one representative protein in each group
523 was selected. From this selection process we found 94 representative proteins from 72
524 bacterial lineages with 23 unique domain architectures.

525

526 *Protein homology search*: We performed homology searches of the 26 non-bacterial DciA
527 proteins using the NCBI BLASTP (40). When examining the results, we excluded any non-
528 bacterial query protein (from the 27) if they retrieved <5% non-bacteria in their top 100 hits (or
529 23 hits in the case of RLI67678.1) (≥95% were bacterial).

530 Analysis using MolEvolvR

531 *Domain architectures*: We used MolEvolvR (39) to determine and characterize all DciA-
532 containing proteins from InterPro and their homologs. We first downloaded the sequences of
533 all DciA-containing proteins identified by InterPro from UniProt. The domain architectures
534 were identified using InterProscan (85) and analyzed by lineage, quantified with heatmaps, and
535 visualized by unique combinations of Pfam domains. During this analysis, we renamed
536 MobiDBLite predictions to "Intrinsically disordered regions" to be consistent with previous
537 literature. Also, DciA homologs with TPR fusions were condensed by the number of TPR
538 repeats for clarity, *e.g.*, TPR+TPR+TPR was condensed to TPR(3). We then aggregated relevant
539 species and protein annotation metadata from the NCBI into our combined dataset. We
540 selected 94 representatives to include each combination of bacterial lineage (excluding
541 atribacterota, which did not contain class-level assignments) and Pfam domain architecture as
542 queries for MolEvolvR homology search.
543
544 *Homology search*: These 94 proteins were submitted to MolEvolvR to identify homologs in the
545 NCBI RefSeq non-redundant proteins database (86). The domain architectures and sequence-
546 structure motif predictions, as well as lineage and protein-related metadata, were determined

547 using MolEvolvR for each of the homologs (as described above) for downstream analyses. The
548 resulting data were summarized and visualized from within MolEvolvR and using custom R
549 scripts.
550
551 *Data availability*: All our data, analyses, and visualizations summarizing the DciA homologs
552 across the bacterial kingdom, along with their domain architectures and phyletic spreads, are
553 available at https://github.com/JRaviLab/dcia_evolution. Detailed legends for our data tables,
554 structure predictions, and sequences used for tree generation are also available in our GitHub
555 repository.
556

557 ## Phylogenetic Tree

558 Fasta sequences of all DciA-containing proteins from InterPro (~27k) were obtained from the
559 UniProtKB. These sequences were aligned using kalign3 (87) and a phylogenetic tree was
560 constructed using FastTree (88). The resulting tree was visualized with FigTree
561 (http://tree.bio.ed.ac.uk/software/figtree/) and color-coded by lineage.
562

563 ## Alphafold Structure Prediction

564 We used the AlphaFold structural prediction Colab notebook (37, 89) via the ChimeraX 1.4 daily
565 build software (90) downloaded 2022-02-07 for all protein models. Visualization and analyses
566 of models performed with UCSF ChimeraX, developed by the Resource for Biocomputing,
567 Visualization, and Informatics at the University of California, San Francisco (90). All AlphaFold

568 structures have been deposited via ModelArchive (http://modelarchive.org/), and are available
569 with the following accession codes (follow the link and enter the temporary supplementary
570 access code when prompted): ma-q8sq3 (*K. uniflora* – temporary supplemental access code:
571 xbO9Q6QacF), ma-vyetl *(H. bicolor E* – temporary supplemental access code: u1N27DoUat),
572 ma-z6rsv *(B. fragilis* – temporary supplemental access code: 16QiFKRCzw), ma-1hvpi *(V.*
573 *cholerae* – temporary supplemental access code: UWLLwXhQa4), ma-tk4v8 *(R. islandica* –
574 temporary supplemental access code: ljFtsjbocW), ma-9cnra *(A. aerolatus* – temporary
575 supplemental access code: uyu5HEqHrF), ma-v2jc1 *(O. acuminata* – temporary supplemental
576 access code: yMKAkPTopL*)*, ma-ibgex *(P. aeruginosa* – temporary supplemental access code:
577 HcHuzHbF4s), ma-20vw9 *(M. tuberculosis* – temporary supplementary access code:
578 kUR6yS2EXW), ma-n7tbg *(L. interrogans* – temporary supplementary access code:
579 R02X0DN45Q), ma-02qnb *(T. maritima* – temporary supplemental access code: LvLPofxN1e),
580 ma-3ee0e *(R. conorii* – temporary supplementary access code: GBBQZBO9LD*)*. Public DOIs
581 (currently pending) will become available upon publication. The structures are also available in
582 our GitHub repository (PDB format; under 'model_structures'):
583 https://github.com/JRaviLab/dcia_evolution.

584 **ACKNOWLEDGEMENTS**

585 We are very grateful to the Midwest Microbial Pathogenesis Conference (MMPC) 2021
586 organizers for providing HCB a travel award and opportunity to present the DciA story. This
587 interactive venue enabled the start of this collaboration between JR, JTB and CLS, HCB.

588

589 **FUNDING**

590 CLS is supported by a Burroughs Wellcome Fund Investigator in the Pathogenesis of Infectious
591 Disease Award. HCB is supported by the Sondra Schlesinger Student Fellowship in Molecular
592 Microbiology. JR is supported by Michigan State University (MSU) College of Veterinary
593 Medicine Endowed Research Funds and MSU start-up funds. UCSF ChimeraX has support from
594 National Institutes of Health R01-GM129325 and the Office of Cyber Infrastructure and
595 Computational Biology, National Institute of Allergy and Infectious Diseases.

596

597 **DATA AVAILABILITY AND REUSE**

598 All the data, analyses, and visualizations are available in our GitHub repository,
599 https://github.com/JRaviLab/dcia_evolution. Text, figures, and data are licensed under
600 Creative Commons Attribution CC BY 4.0.

601

602 **REFERENCES**

603 1. Chodavarapu S, Kaguni JM. 2016. Replication Initiation in Bacteria. Enzymes 39:1–30.

604 2. Fuller RS, Funnell BE, Kornberg A. 1984. The dnaA protein complex with the E. coli
605 chromosomal replication origin (oriC) and other DNA sites. Cell 38:889–900.

606 3. Fuller RS, Kornberg A. 1983. Purified dnaA protein in initiation of replication at the
607 Escherichia coli chromosomal origin of replication. Proceedings of the National Academy
608 of Sciences 80:5817-5821.

609 4. Jameson KH, Wilkinson AJ. 2017. Control of Initiation of DNA Replication in Bacillus
610 subtilis and Escherichia coli. Genes 8:22–22.

611 5. Kaguni JM. 2011. Replication initiation at the Escherichia coli chromosomal origin.
612 Current opinion in chemical biology, 2011/08/18 ed. 15:606–613.

613 6. Mott ML, Berger JM. 2007. DNA replication initiation: mechanisms and regulation in
614 bacteria. Nature Reviews Microbiology 5:343–354.

615 7. Schaper S, Messer W. 1995. Interaction of the initiator protein DnaA of Escherichia coli
616 with its DNA target. The Journal of biological chemistry 270:17622–17626.

617 8. O'Donnell M, Langston L, Stillman B. 2013. Principles and concepts of DNA replication in
618 bacteria, archaea, and eukarya. Cold Spring Harbor perspectives in biology 5:a010108–
619 a010108.

620 9. Bramhill D, Kornberg A. 1988. Duplex opening by dnaA protein at novel sequences in
621 initiation of replication at the origin of the E. coli chromosome. Cell 52:743–755.

622 10. Meyer RR, Laine PS. 1990. The single-stranded DNA-binding protein of Escherichia coli.
623 Microbiological reviews 54:342–380.

624 11. Baker TA, Funnell BE, Kornberg A. 1987. Helicase action of dnaB protein during
625 replication from the Escherichia coli chromosomal origin in vitro. Journal of Biological
626 Chemistry 262:6877–6885.

627 12. LeBowitz JH, McMacken R. 1986. The Escherichia coli dnaB replication protein is a DNA
628 helicase. The Journal of biological chemistry 261:4738–4748.

629 13. Lewis JS, Jergic S, Dixon NE. 2016. The E. coli DNA Replication Fork. The Enzymes 39:31–
630 88.

631 14. Oakley AJ. 2019. A structural view of bacterial DNA replication. Protein science: a
632 publication of the Protein Society 28:990–1004.

633 15. Gorbalenya AE, Koonin EV. 1993. Helicases: amino acid sequence comparisons and
634 structure-function relationships. Current Opinion in Structural Biology 3:419–429.

635 16. Leipe DD, Aravind L, Grishin NV, Koonin EV. 2000. The bacterial replicative helicase DnaB
636 evolved from a RecA duplication. Genome research 10:5–16.

637 17. Fernandez AJ, Berger JM. 2021. Mechanisms of hexameric helicases. Critical Reviews in
638 Biochemistry and Molecular Biology 56:621–639.

639 18. Itsathitphaisarn O, Wing RA, Eliason WK, Wang J, Steitz TA. 2012. The hexameric helicase
640 DnaB adopts a nonplanar conformation during translocation. Cell 151:267–277.

641 19. Spinks RR, Spenkelink LM, Stratmann SA, Xu Z-Q, Stamford NPJ, Brown SE, Dixon NE,
642 Jergic S, van Oijen AM. 2021. DnaB helicase dynamics in bacterial DNA replication
643 resolved by single-molecule studies. Nucleic acids research 49:6804–6816.

644 20. Nakayama N, Arai N, Kaziro Y, Arai K. 1984. Structural and functional studies of the dnaB
645 protein using limited proteolysis. Characterization of domains for DNA-dependent ATP

646 hydrolysis and for protein association in the primosome. The Journal of biological
647 chemistry 259:88–96.

648 21. Sakamoto Y, Nakai S, Moriya S, Yoshikawa H, Ogasawara N. 1995. The Bacillus subtilis
649 dnaC gene encodes a protein homologous to the DnaB helicase of Escherichia coli.
650 Microbiology (Reading, England) 141(Pt 3):641–644.

651 22. Arias-Palomo E, Puri N, O'Shea Murray VL, Yan Q, Berger JM. 2019. Physical Basis for the
652 Loading of a Bacterial Replicative Helicase onto DNA. Molecular cell 74:173-184.e4.

653 23. Liu B, Eliason WK, Steitz TA. 2013. Structure of a helicase–helicase loader complex
654 reveals insights into the mechanism of bacterial primosome assembly. Nat Commun
655 4:2495.

656 24. Bruand C, Farache M, McGovern S, Ehrlich SD, Polard P. 2001. DnaB, DnaD and DnaI
657 proteins are components of the Bacillus subtilis replication restart primosome. Molecular
658 microbiology 42:245–255.

659 25. Kobori JA, Kornberg A. 1982. The Escherichia coli dnaC gene product. II. Purification,
660 physical properties, and role in replication. Journal of Biological Chemistry 257:13763–
661 13769.

662 26. Koonin EV. 1992. DnaC protein contains a modified ATP-binding motif and belongs to a
663 novel family of ATPases including also DnaA. Nucleic acids research 20:1997–1997.

664 27. Wahle E, Lasken RS, Kornberg A. 1989. The dnaB-dnaC replication protein complex of
665 Escherichia coli. II. Role of the complex in mobilizing dnaB functions. J Biol Chem
666 264:2469–2475.

667 28. Brézellec P, Vallet-Gely I, Possoz C, Quevillon-Cheruel S, Ferat J-L. 2016. DciA is an
668 ancestral replicative helicase operator essential for bacterial replication initiation. Nat
669 Commun 7:13271.

670 29. Chase J, Berger J, Jeruzalmi D. 2022. Convergent evolution in two bacterial replicative
671 helicase loaders. Trends in Biochemical Sciences 26:S0968-0004(22)00042-1.

672 30. Rokop ME, Auchtung JM, Grossman AD. 2004. Control of DNA replication initiation by
673 recruitment of an essential initiation protein to the membrane of Bacillus subtilis. Mol
674 Microbiol 52:1757–1767.

675 31. Weigel C, Seitz H. 2006. Bacteriophage replication modules. FEMS Microbiol Rev 30:321–
676 381.

677 32. Davey MJ, Fang L, McInerney P, Georgescu RE, O'Donnell M. 2002. The DnaC helicase
678 loader is a dual ATP/ADP switch protein. EMBO J 21:3148–3159.

679 33. Ioannou C, Schaeffer PM, Dixon NE, Soultanas P. 2006. Helicase binding to DnaI exposes
680 a cryptic DNA-binding site during helicase loading in Bacillus subtilis. Nucleic Acids Res
681 34:5247–5258.

682 34. Mann KM, Huang DL, Hooppaw AJ, Logsdon MM, Richardson K, Lee HJ, Kimmey JM,
683 Aldridge BB, Stallings CL. 2017. Rv0004 is a new essential member of the mycobacterial
684 DNA replication machinery. PLoS Genet 13:e1007115.

685 35. Chan-Yao-Chong M, Marsin S, Quevillon-Cheruel S, Durand D, Ha-Duong T. 2020.
686 Structural ensemble and biological activity of DciA intrinsically disordered region. Journal
687 of Structural Biology 212:107573.

688 36. Marsin S, Adam Y, Cargemel C, Andreani J, Baconnais S, Legrand P, Li de la Sierra-Gallay
689 I, Humbert A, Aumont-Nicaise M, Velours C, Ochsenbein F, Durand D, Le Cam E, Walbott
690 H, Possoz C, Quevillon-Cheruel S, Ferat J-L. 2021. Study of the DnaB:DciA interplay
691 reveals insights into the primary mode of loading of the bacterial replicative helicase.
692 Nucleic Acids Research 49:6569-6586.

693 37. Jumper J, Evans R, Pritzel A, Green T, Figurnov M, Ronneberger O, Tunyasuvunakool K,
694 Bates R, Žídek A, Potapenko A, Bridgland A, Meyer C, Kohl SAA, Ballard AJ, Cowie A,
695 Romera-Paredes B, Nikolov S, Jain R, Adler J, Back T, Petersen S, Reiman D, Clancy E,
696 Zielinski M, Steinegger M, Pacholska M, Berghammer T, Bodenstein S, Silver D, Vinyals
697 O, Senior AW, Kavukcuoglu K, Kohli P, Hassabis D. 2021. Highly accurate protein
698 structure prediction with AlphaFold. 7873. Nature 596:583–589.

699 38. Blum M, Chang H-Y, Chuguransky S, Grego T, Kandasaamy S, Mitchell A, Nuka G,
700 Paysan-Lafosse T, Qureshi M, Raj S, Richardson L, Salazar GA, Williams L, Bork P, Bridge
701 A, Gough J, Haft DH, Letunic I, Marchler-Bauer A, Mi H, Natale DA, Necci M, Orengo CA,

702 Pandurangan AP, Rivoire C, Sigrist CJA, Sillitoe I, Thanki N, Thomas PD, Tosatto SCE, Wu
703 CH, Bateman A, Finn RD. 2021. The InterPro protein families and domains database: 20
704 years on. Nucleic Acids Research 49:D344–D354.

705 39. Burke JT, Chen SZ, Sosinski LM, Johnston JB, Ravi J. 2022. MolEvolvR: A web-app for
706 characterizing proteins using molecular evolution and phylogeny. bioRxiv
707 https://doi.org/10.1101/2022.02.18.461833.

708 40. Altschul SF, Gish W, Miller W, Myers EW, Lipman DJ. 1990. Basic local alignment search
709 tool. J Mol Biol 215:403–410.

710 41. Sun Y, Deng T, Zhang A, Moore MJ, Landis JB, Lin N, Zhang H, Zhang X, Huang J, Zhang
711 X, Sun H, Wang H. 2020. Genome Sequencing of the Endangered Kingdonia uniflora
712 (Circaeasteraceae, Ranunculales) Reveals Potential Mechanisms of Evolutionary
713 Specialization. iScience 23:101124.

714 42. Arnesano F, Banci L, Bertini I, Ciofi-Baffoni S, Molteni E, Huffman DL, O'Halloran TV.
715 2002. Metallochaperones and Metal-Transporting ATPases: A Comparative Analysis of
716 Sequences and Structures. Genome Res 12:255–271.

717 43. Dykema PE, Sipes PR, Marie A, Biermann BJ, Crowell DN, Randall SK. 1999. A new class
718 of proteins capable of binding transition metals. Plant Mol Biol 41:139–150.

719 44. Sun X-H, Yu G, Li J-T, Jia P, Zhang J-C, Jia C-G, Zhang Y-H, Pan H-Y. 2014. A Heavy Metal-
720 Associated Protein (AcHMA1) from the Halophyte, Atriplex canescens (Pursh) Nutt.,

721 Confers Tolerance to Iron and Other Abiotic Stresses When Expressed in Saccharomyces
722 cerevisiae. Int J Mol Sci 15:14891–14906.

723 45. Morales ME, Derbes RS, Ade CM, Ortego JC, Stark J, Deininger PL, Roy-Engel AM. 2016.
724 Heavy Metal Exposure Influences Double Strand Break DNA Repair Outcomes. PLoS ONE
725 11:e0151367.

726 46. Stohs SJ, Bagchi D. 1995. Oxidative mechanisms in the toxicity of metal ions. Free Radic
727 Biol Med 18:321–336.

728 47. Zhou S, Wei C, Liao C, Wu H. 2008. Damage to DNA of effective microorganisms by heavy
729 metals: Impact on wastewater treatment. Journal of Environmental Sciences 20:1514–
730 1518.

731 48. Blackwell GA, Hunt M, Malone KM, Lima L, Horesh G, Alako BTF, Thomson NR, Iqbal Z.
732 2021. Exploring bacterial diversity via a curated and searchable snapshot of archived DNA
733 sequences. PLoS biology 19:e3001421–e3001421.

734 49. Land M, Hauser L, Jun S-R, Nookaew I, Leuze MR, Ahn T-H, Karpinets T, Lund O, Kora G,
735 Wassenaar T, Poudel S, Ussery DW. 2015. Insights from 20 years of bacterial genome
736 sequencing. Functional & integrative genomics 15:141–161.

737 50. Tatusova T, Ciufo S, Fedorov B, O'Neill K, Tolstoy I. 2014. RefSeq microbial genomes
738 database: new representation and annotation strategy. Nucleic Acids Research 42:D553–
739 D559.

740 51. Atkinson HJ, Babbitt PC. 2009. An atlas of the thioredoxin fold class reveals the
741 complexity of function-enabling adaptations. PLoS Comput Biol 5:e1000541.

742 52. Lee S, Kim SM, Lee RT. 2013. Thioredoxin and Thioredoxin Target Proteins: From
743 Molecular Mechanisms to Functional Significance. Antioxid Redox Signal 18:1165–1207.

744 53. Lu J, Holmgren A. 2014. The Thioredoxin Superfamily in Oxidative Protein Folding.
745 Antioxidants & Redox Signaling 21:457–470.

746 54. Goemans CV, Beaufay F, Wahni K, Van Molle I, Messens J, Collet J-F. 2018. An essential
747 thioredoxin is involved in the control of the cell cycle in the bacterium Caulobacter
748 crescentus. J Biol Chem 293:3839–3848.

749 55. Muley VY, Akhter Y, Galande S. 2019. PDZ Domains Across the Microbial World:
750 Molecular Link to the Proteases, Stress Response, and Protein Synthesis. Genome
751 Biology and Evolution 11:644–659.

752 56. Nourry C, Grant SGN, Borg J-P. 2003. PDZ domain proteins: plug and play! Sci STKE
753 (179):RE7.

754 57. Kojima Y, Machida Y, Palani S, Caulfield TR, Radisky ES, Kaufmann SH, Machida YJ. 2020.
755 FAM111A protects replication forks from protein obstacles via its trypsin-like domain. Nat
756 Commun 11:1318.

757 58. Burroughs AM, Zhang D, Schäffer DE, Iyer LM, Aravind L. 2015. Comparative genomic
758 analyses reveal a vast, novel network of nucleotide-centric systems in biological conflicts,
759 immunity and signaling. Nucleic acids research, 2015/11/20 ed. 43:10633–10654.

760 59. Cordin O, Banroques J, Tanner NK, Linder P. 2006. The DEAD-box protein family of RNA
761 helicases. Gene 367:17–37.

762 60. Wyszomirski KH, Curth U, Alves J, Mackeldanz P, Möncke-Buchner E, Schutkowski M,
763 Krüger DH, Reuter M. 2012. Type III restriction endonuclease EcoP15I is a heterotrimeric
764 complex containing one Res subunit with several DNA-binding regions and ATPase
765 activity. Nucleic Acids Res 40:3610–3622.

766 61. Britton RA, Lin DC-H, Grossman AD. 1998. Characterization of a prokaryotic SMC protein
767 involved in chromosome partitioning. Genes Dev 12:1254–1259.

768 62. Hirano T. 2005. SMC proteins and chromosome mechanics: from bacteria to humans.
769 Philos Trans R Soc Lond B Biol Sci 360:507–514.

770 63. Pellegrino S, Radzimanowski J, de Sanctis D, Boeri Erba E, McSweeney S, Timmins J.
771 2012. Structural and functional characterization of an SMC-like protein RecN: new
772 insights into double-strand break repair. Structure 20:2076–2089.

773 64. Strunnikov AV, Jessberger R. 1999. Structural maintenance of chromosomes (SMC)
774 proteins. European Journal of Biochemistry 263:6–13.

775 65. Strunnikov AV. 2006. SMC complexes in bacterial chromosome condensation and
776 segregation. Plasmid 55:135–144.

777 66. Kelch BA, Makino DL, O'Donnell M, Kuriyan J. 2012. Clamp loader ATPases and the
778 evolution of DNA replication machinery. BMC Biology 10:34.

779 67. O'Donnell M, Jeruzalmi D, Kuriyan J. 2001. Clamp loader structure predicts the
780 architecture of DNA polymerase III holoenzyme and RFC. Current Biology 11:R935–R946.

781 68. Zeytuni N, Zarivach R. 2012. Structural and Functional Discussion of the Tetra-Trico-
782 Peptide Repeat, a Protein Interaction Module. Structure 20:397–405.

783 69. Morohashi H, Maculins T, Labib K. 2009. The Amino-Terminal TPR Domain of Dia2
784 Tethers SCFDia2 to the Replisome Progression Complex. Current Biology 19:1943–1949.

785 70. Bang S, Min C-K, Ha N-Y, Choi M-S, Kim I-S, Kim Y-S, Cho N-H. 2016. Inhibition of
786 eukaryotic translation by tetratricopeptide-repeat proteins of Orientia tsutsugamushi. J
787 Microbiol 54:136–144.

788 71. Alfieri C, Zhang S, Barford D. 2017. Visualizing the complex functions and mechanisms of
789 the anaphase promoting complex/cyclosome (APC/C). Open Biol 7:170204.

790 72. Sudakin V, Ganoth D, Dahan A, Heller H, Hershko J, Luca FC, Ruderman JV, Hershko A.
791 1995. The cyclosome, a large complex containing cyclin-selective ubiquitin ligase activity,
792 targets cyclins for destruction at the end of mitosis. Mol Biol Cell 6:185–197.

793 73. Cozzarelli NR. 1980. DNA Gyrase and the Supercoiling of DNA. Science 207:953–960.

794 74. Antony E, Lohman TM. 2019. Dynamics of E. coli single stranded DNA binding (SSB)
795 protein-DNA complexes. Seminars in cell & developmental biology 86:102–111.

796 75. Bianco PR, Pottinger S, Tan HY, Nguyenduc T, Rex K, Varshney U. 2017. The IDL of E. coli
797 SSB links ssDNA and protein binding by mediating protein-protein interactions. Protein
798 science: a publication of the Protein Society 26:227–241.

799 76. Kozlov AG, Weiland E, Mittal A, Waldman V, Antony E, Fazio N, Pappu RV, Lohman TM.
800 2015. Intrinsically Disordered C-Terminal Tails of E. coli Single-Stranded DNA Binding
801 Protein Regulate Cooperative Binding to Single-Stranded DNA. Journal of Molecular
802 Biology 427:763–774.

803 77. Tan HY, Wilczek LA, Pottinger S, Manosas M, Yu C, Nguyenduc T, Bianco PR. 2017. The
804 intrinsically disordered linker of E. coli SSB is critical for the release from single-stranded
805 DNA. Protein science: a publication of the Protein Society 26:700–717.

806 78. Guy CP, Atkinson J, Gupta MK, Mahdi AA, Gwynn EJ, Rudolph CJ, Moon PB, van
807 Knippenberg IC, Cadman CJ, Dillingham MS, Lloyd RG, McGlynn P. 2009. Rep Provides a
808 Second Motor at the Replisome to Promote Duplication of Protein-Bound DNA.
809 Molecular Cell 36:654–666.

810 79. Nguyen B, Shinn MK, Weiland E, Lohman TM. 2021. Regulation of E. coli Rep helicase
811 activity by PriC. Journal of Molecular Biology 433:167072–167072.

812 80. Necci M, Piovesan D, Dosztányi Z, Tosatto SCE. 2017. MobiDB-lite: fast and highly
813 specific consensus prediction of intrinsic disorder in proteins. Bioinformatics (Oxford,
814 England) 33:1402–1404.

815 81. Jameson KH, Rostami N, Fogg MJ, Turkenburg JP, Grahl A, Murray H, Wilkinson AJ. 2014.
816 Structure and interactions of the Bacillus subtilis sporulation inhibitor of DNA replication,
817 SirA, with domain I of DnaA. Mol Microbiol 93:975–991.

818 82. Abe Y, Jo T, Matsuda Y, Matsunaga C, Katayama T, Ueda T. 2007. Structure and function
819 of DnaA N-terminal domains: specific sites and mechanisms in inter-DnaA interaction and
820 in DnaB helicase loading on oriC. The Journal of biological chemistry 282:17816–17827.

821 83. Sutton MD, Carr KM, Vicente M, Kaguni JM. 1998. Escherichia coli DnaA protein. The N-
822 terminal domain and loading of DnaB helicase at the E. coli chromosomal origin. J Biol
823 Chem 273:34255–34262.

824 84. Keyamura K, Abe Y, Higashi M, Ueda T, Katayama T. 2009. DiaA dynamics are coupled
825 with changes in initial origin complexes leading to helicase loading. The Journal of
826 biological chemistry 284:25038–25050.

827 85. InterProScan 5: genome-scale protein function classification. Bioinformatics 30(9):1236-
828 1240.

829 86. O'Leary NA, Wright MW, Brister JR, Ciufo S, Haddad D, McVeigh R, Rajput B, Robbertse
830 B, Smith-White B, Ako-Adjei D, Astashyn A, Badretdin A, Bao Y, Blinkova O, Brover V,
831 Chetvernin V, Choi J, Cox E, Ermolaeva O, Farrell CM, Goldfarb T, Gupta T, Haft D,

832 Hatcher E, Hlavina W, Joardar VS, Kodali VK, Li W, Maglott D, Masterson P, McGarvey
833 KM, Murphy MR, O'Neill K, Pujar S, Rangwala SH, Rausch D, Riddick LD, Schoch C,
834 Shkeda A, Storz SS, Sun H, Thibaud-Nissen F, Tolstoy I, Tully RE, Vatsan AR, Wallin C,
835 Webb D, Wu W, Landrum MJ, Kimchi A, Tatusova T, DiCuccio M, Kitts P, Murphy TD,
836 Pruitt KD. 2016. Reference sequence (RefSeq) database at NCBI: current status,
837 taxonomic expansion, and functional annotation. Nucleic acids research 44:D733-45.

838 87. Lassmann T. 2020. Kalign 3: multiple sequence alignment of large datasets.
839 Bioinformatics 36:1928–1929.

840 88. Price MN, Dehal PS, Arkin AP. 2009. FastTree: Computing Large Minimum Evolution
841 Trees with Profiles instead of a Distance Matrix. Molecular Biology and Evolution
842 26:1641–1650.

843 89. Varadi M, Anyango S, Deshpande M, Nair S, Natassia C, Yordanova G, Yuan D, Stroe O,
844 Wood G, Laydon A, Žídek A, Green T, Tunyasuvunakool K, Petersen S, Jumper J, Clancy
845 E, Green R, Vora A, Lutfi M, Figurnov M, Cowie A, Hobbs N, Kohli P, Kleywegt G, Birney E,
846 Hassabis D, Velankar S. 2022. AlphaFold Protein Structure Database: massively
847 expanding the structural coverage of protein-sequence space with high-accuracy models.
848 Nucleic Acids Research 50:D439–D444.

849 90. Pettersen EF, Goddard TD, Huang CC, Meng EC, Couch GS, Croll TI, Morris JH, Ferrin TE.
850 2021. UCSF ChimeraX: Structure visualization for researchers, educators, and developers.
851 Protein Sci 30:70–82.

852

853 # FIGURE LEGENDS

854 **Figure 1. DciA protein phyletic spread and domain architectures. A.** Phyletic spread of DciA
855 domain containing proteins. The heatmap shows the abundance of DciA containing proteins
856 across Bacterial, Archaeal, Viral, and Eukaryotic lineages. The color gradient indicates the
857 number of homologs in a particular lineage. **B.** Phyletic spread of diverse DciA domain
858 architectures (excluding DciA single-domain proteins) across bacterial lineages. The color
859 gradient indicates the number of homologs with that domain architecture in a particular
860 lineage. Domain architectures involving TPR repeats were combined based on the number of
861 repeats. **C.** Key domain architectures of bacterial DciA homologs (including Pfam domains and
862 MobiDBLite predicted IDRs). Representative proteins for each Pfam domain architecture
863 within annotated bacterial lineages (no candidatus or metagenomes) were selected. Each
864 representative protein is marked with the kingdom (B, bacteria), phylum (first 6 letters),
865 Genus, and species (represented as 'Gspecies'), and the NCBI protein accession number. The
866 Pfam and MobiDB annotations for each domain prediction are shown in the legend. The arrow
867 lengths represent the overall protein length. The characteristic DciA domain is indicated with a
868 black arrow in the legend (grey domains).

869

870 **Figure 2. Length and DciA domain positioning in DciA single-domain proteins. A.**
871 Distributions of DciA single-domain protein length and the distances of the DciA domain from
872 the N and C termini across bacterial lineages. Summary statistics for the single-domain DciA

873 proteins were calculated for all bacterial lineages (no candidatus or metagenomes). The blue
874 lines represent the 25th and 75th (light blue), and median/50th (dark blue) percentiles across
875 lineages. **B.** AlphaFold structural prediction on the *B. fragilis* (AUI45441.1) and *V. cholerae*
876 (AAF95538.1) DciA proteins visualized with ChimeraX. Protein is oriented left-to-right N-C
877 termini. Color key indicates accuracy confidence (0–100).
878
879 **Figure 3. Disordered regions in DciA single-domain proteins. A.** Phyletic spreads of
880 Intrinsically disordered region (IDR)-containing DciA proteins. The heatmap shows the
881 abundance of IDR-containing DciA proteins across bacterial lineages (no candidatus or
882 metagenomes). 'x' in 'IDR(x)' indicates the number of IDRs predicted. The color gradient
883 indicates the number of homologs in a particular lineage. **B.** Distribution of IDR length across
884 bacterial lineages. Summary statistics for the single-domain DciA proteins with IDRs were
885 calculated and plotted for each bacterial lineage. The blue lines represent the 25th and 75th
886 (light blue), and median/50th (dark blue) percentiles across lineages.
887
888 **Figure 4. Grouping of DciA single-domain proteins and their phyletic spread.** The top panel
889 shows the four Groups of bacterial DciA single-domain proteins binned based on the lengths of
890 flanking N- and C-terminal extensions of DciA domains: : i) Group 1 proteins with ≥14aa N-
891 terminal to the DciA domain and <14aa C-terminal, ii) Group 2 proteins with <14aa N-terminal
892 to the DciA domain and ≥14aa C-terminal, iii) Group 3 proteins with ≥14aa both N- and C-
893 terminally to the DciA domain, and iv) Group 4 proteins with <14aa on both N- and C-termini.
894 Stacked barplots of 4 groups of DciA single-domain proteins are plotted across **A.** all bacterial

895 lineages, with a focus on **B.** predominant lineages further resolved into sub-phyla
896 (proteobacteria, actinobacteria, and bacteroidetes), and **C.** other lineages. The number of
897 homologs in each group is are further characterized based on their lineage-wise distribution.
898 No bacterial candidatus or metagenomes are displayed.
899
900 **Figure 5. Structure prediction of representative DciA homologs by groups (with and**
901 **without IDR).** AlphaFold representatives from **A.** Group 1 DciA proteins from *A. aerolatus* (left;
902 GEO04242.1) and *R. islandica* (right; KLU02380.1), **B.** Group 2 DciA proteins from *P. aeruginosa*
903 (left; AAG07793.1) and *O. acuminata* (right; AFY85399.1), **C.** Group 3 DciA proteins from *L.*
904 *interrogans* (left; AAN47203.1) and *M. tuberculosis* (right; BAL63824.1), and Group 4 DciA
905 proteins *T. maritima* (left; AAD35914.1) and *R. conorii* (right; AAL03818.1). Models visualized
906 with ChimeraX. Proteins are oriented left-to-right N-C termini, termini marked on each
907 structure. DciA domains annotated in blue text, IDRs annotated with black bracket with all
908 corresponding amino acid annotations. Key indicates accuracy confidence (0–100). See
909 *Methods* for accession codes of each model deposited in ModelArchive.
910
911 **Figure 6. DciA evolution across the tree of life.** All DciA domain-containing proteins from
912 Figure 1 were used to reconstruct the DciA phylogenetic tree. Kalign3 (87) was used for
913 multiple sequence alignment, and FastTree (88) was used to generate the tree. The resulting
914 tree was visualized using FigTree (http://tree.bio.ed.ac.uk/software/figtree/). The tree was
915 colored by major lineages (left: bacterial phyla; right: key bacterial classes) with the remaining
916 DciA proteins in black. The three predominant bacterial lineages, proteobacteria,

917 actinobacteria, and bacteroidetes, are marked on the phylum-based tree **(A)** next to their

918 corresponding largest clusters, and the major bacterial classes are marked next to their largest

919 clusters in the class-based tree **(B)**.

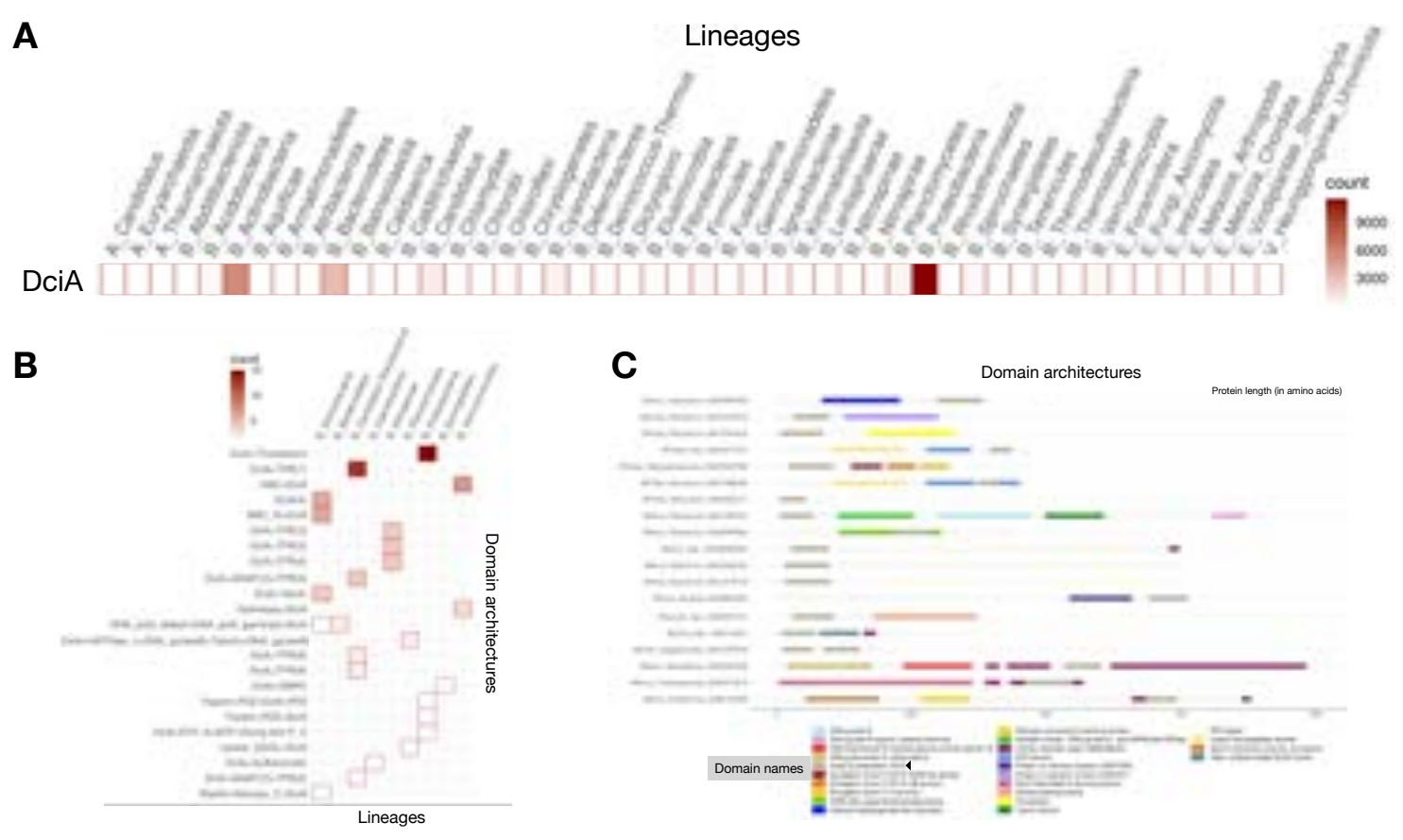
A
Lineages
DciA
count
9000
6000
3000
B
count
Domain architectures
Lineages
C
Domain architectures
Protein length (in amino acids)
Domain names

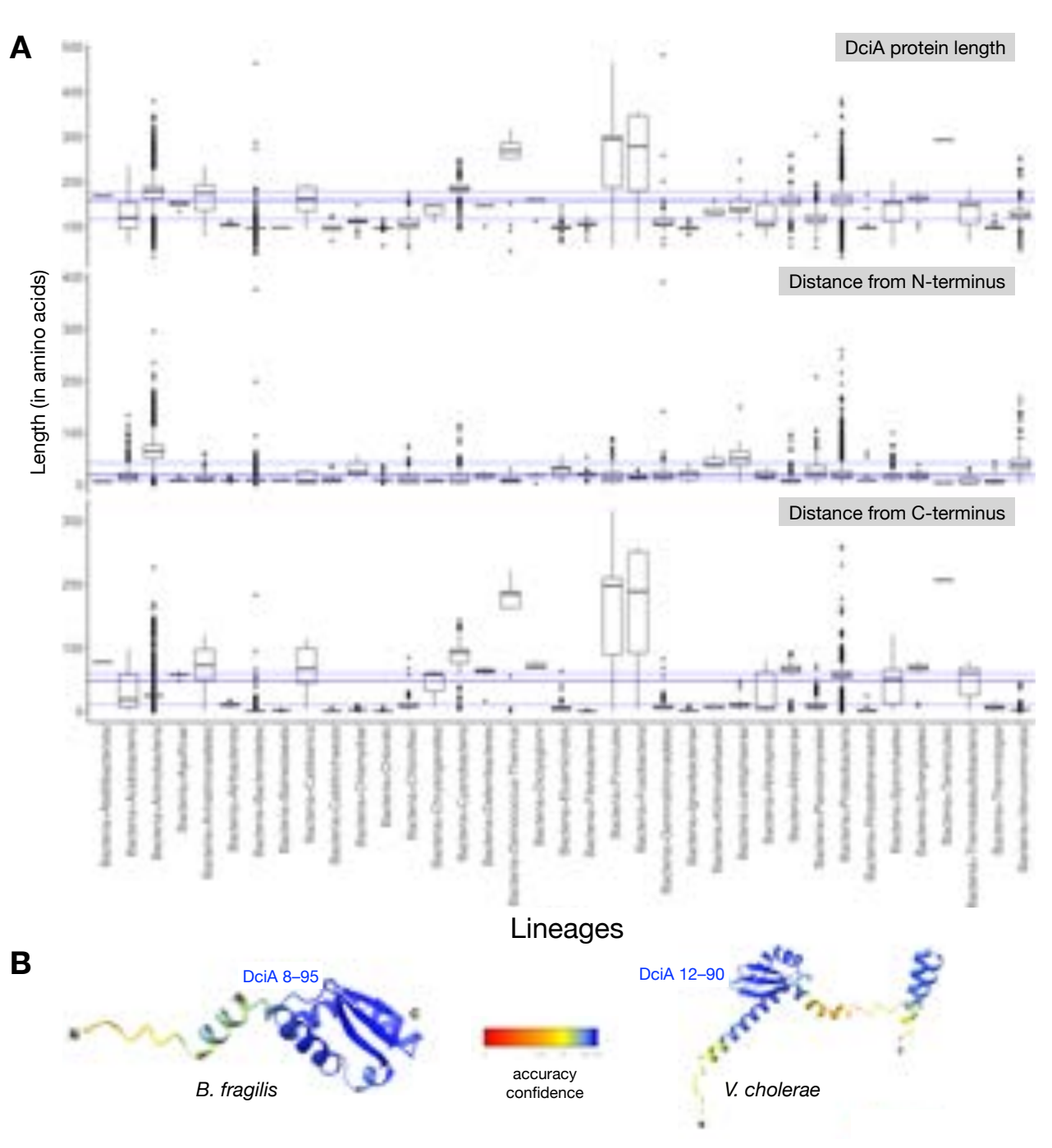
A
DciA protein length
Distance from N-terminus
Distance from C-terminus
Length (in amino acids)
Lineages
B
DciA 8–95
B. fragilis
accuracy
confidence
DciA 12–90
V. cholerae

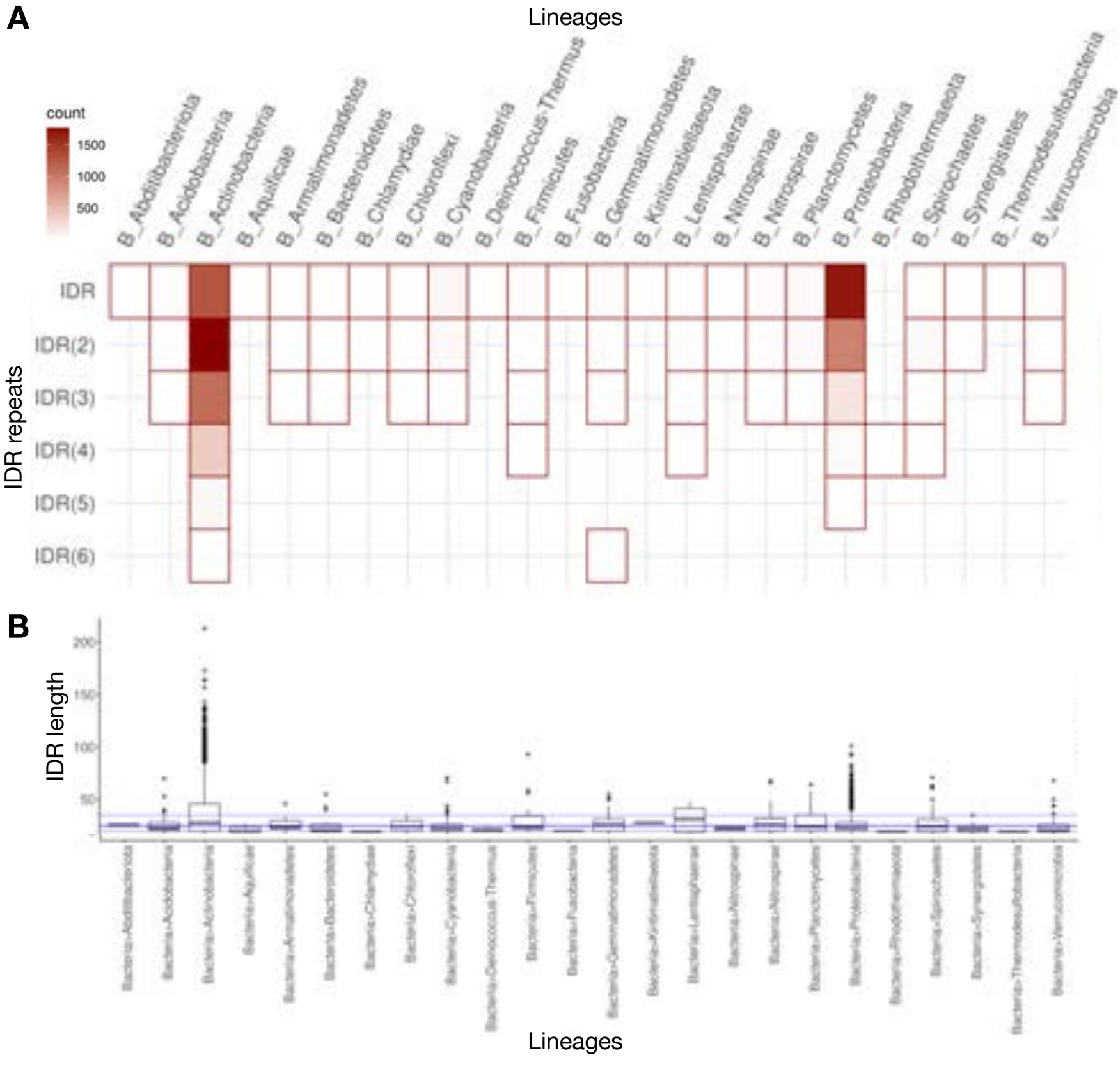
A
Lineages
count
1500
1000
500
B_Abditibacteriota
B_Acidobacteria
B_Actinobacteria
B_Aquificae
B_Armatimonadetes
B_Bacteroidetes
B_Chlamydiae
B_Chloroflexi
B_Cyanobacteria
B_Deinococcus-Thermus
B_Firmicutes
B_Fusobacteria
B_Gemmatimonadetes
B_Kiritimatiellaeota
B_Lentisphaerae
B_Nitrospinae
B_Nitrospirae
B_Planctomycetes
B_Proteobacteria
B_Rhodothermaeota
B_Spirochaetes
B_Synergistetes
B_Thermodesulfobacteria
B_Verrucomicrobia
IDR repeats
IDR
IDR(2)
IDR(3)
IDR(4)
IDR(5)
IDR(6)
B
IDR length
200
150
100
50
Lineages

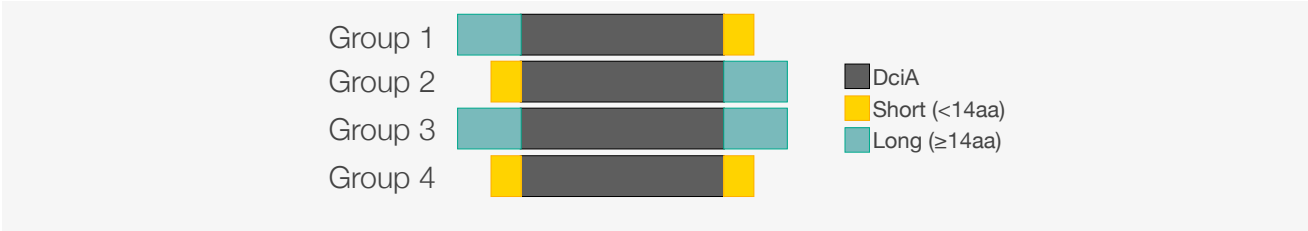
Group 1
Group 2
Group 3
Group 4
DciA
Short (<14aa)
Long (≥14aa)

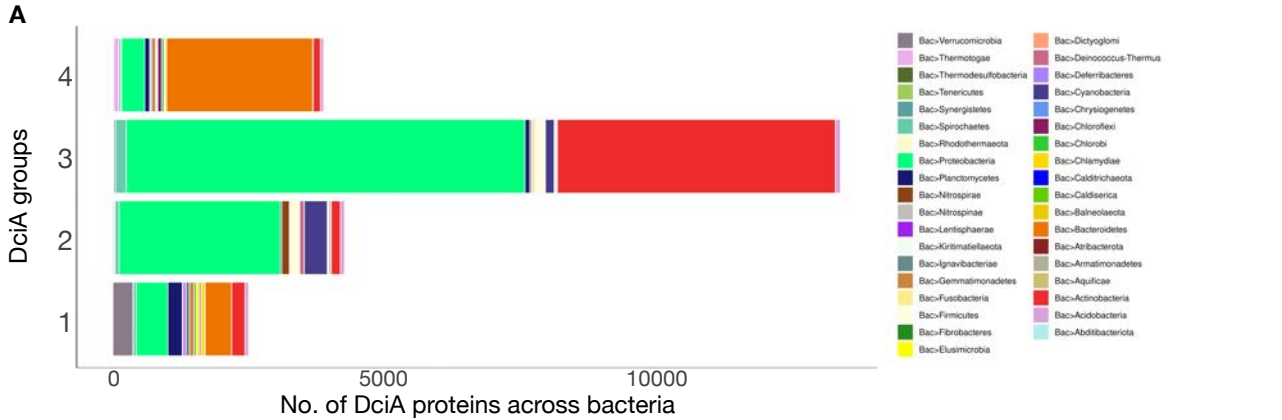
A
DciA groups
4
3
2
1
0
5000
10000
No. of DciA proteins across bacteria
Bac>Verrucomicrobia
Bac>Thermotogae
Bac>Thermodesulfobacteria
Bac>Tenericutes
Bac>Synergistetes
Bac>Spirochaetes
Bac>Rhodothermaeota
Bac>Proteobacteria
Bac>Planctomycetes
Bac>Nitrospirae
Bac>Nitrospinae
Bac>Lentisphaerae
Bac>Kiritimatiellaeota
Bac>Ignavibacteriae
Bac>Gemmatimonadetes
Bac>Fusobacteria
Bac>Firmicutes
Bac>Fibrobacteres
Bac>Elusimicrobia
Bac>Dictyoglomi
Bac>Deinococcus-Thermus
Bac>Deferribacteres
Bac>Cyanobacteria
Bac>Chrysiogenetes
Bac>Chloroflexi
Bac>Chlorobi
Bac>Chlamydiae
Bac>Caldithrichaeota
Bac>Caldiserica
Bac>Balneolaeota
Bac>Bacteroidetes
Bac>Atribacterota
Bac>Armatimonadetes
Bac>Aquificae
Bac>Actinobacteria
Bac>Acidobacteria
Bac>Abditibacteriota

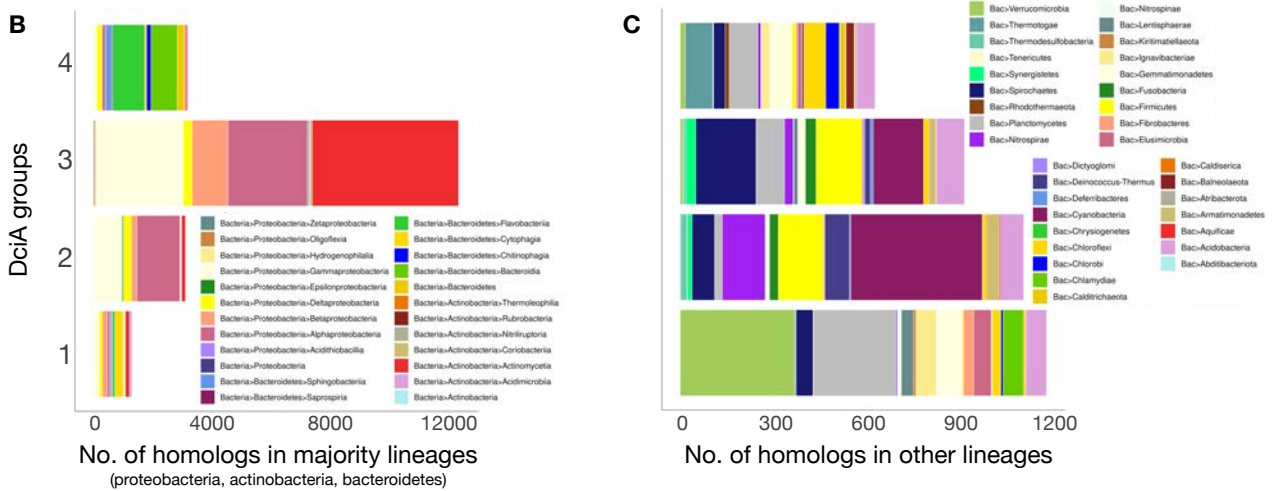
B
DciA groups
4
3
2
1
0
4000
8000
12000
No. of homologs in majority lineages
(proteobacteria, actinobacteria, bacteroidetes)
Bacteria>Proteobacteria>Zetaproteobacteria
Bacteria>Proteobacteria>Oligoflexia
Bacteria>Proteobacteria>Hydrogenophilalia
Bacteria>Proteobacteria>Gammaproteobacteria
Bacteria>Proteobacteria>Epsilonproteobacteria
Bacteria>Proteobacteria>Deltaproteobacteria
Bacteria>Proteobacteria>Betaproteobacteria
Bacteria>Proteobacteria>Alphaproteobacteria
Bacteria>Proteobacteria>Acidithiobacillia
Bacteria>Proteobacteria
Bacteria>Bacteroidetes>Sphingobacteria
Bacteria>Bacteroidetes>Saprospiria
Bacteria>Bacteroidetes>Flavobacteria
Bacteria>Bacteroidetes>Cytophagia
Bacteria>Bacteroidetes>Chitinophagia
Bacteria>Bacteroidetes>Bacteroidia
Bacteria>Bacteroidetes
Bacteria>Actinobacteria>Thermoleophilia
Bacteria>Actinobacteria>Rubrobacteria
Bacteria>Actinobacteria>Nitriliruptoria
Bacteria>Actinobacteria>Coriobacteria
Bacteria>Actinobacteria>Actinomycetia
Bacteria>Actinobacteria>Acidimicrobia
Bacteria>Actinobacteria
C
0
300
600
900
1200
No. of homologs in other lineages
Bac>Verrucomicrobia
Bac>Thermotogae
Bac>Thermodesulfobacteria
Bac>Tenericutes
Bac>Synergistetes
Bac>Spirochaetes
Bac>Rhodothermaeota
Bac>Planctomycetes
Bac>Nitrospirae
Bac>Nitrospinae
Bac>Lentisphaerae
Bac>Kiritimatiellaeota
Bac>Ignavibacteriae
Bac>Gemmatimonadetes
Bac>Fusobacteria
Bac>Firmicutes
Bac>Fibrobacteres
Bac>Elusimicrobia
Bac>Dictyoglomi
Bac>Deinococcus-Thermus
Bac>Deferribacteres
Bac>Cyanobacteria
Bac>Chrysiogenetes
Bac>Chloroflexi
Bac>Chlorobi
Bac>Chlamydiae
Bac>Caldithrichaeota
Bac>Caldiserica
Bac>Balneolaeota
Bac>Atribacterota
Bac>Armatimonadetes
Bac>Aquificae
Bac>Acidobacteria
Bac>Abditibacteriota

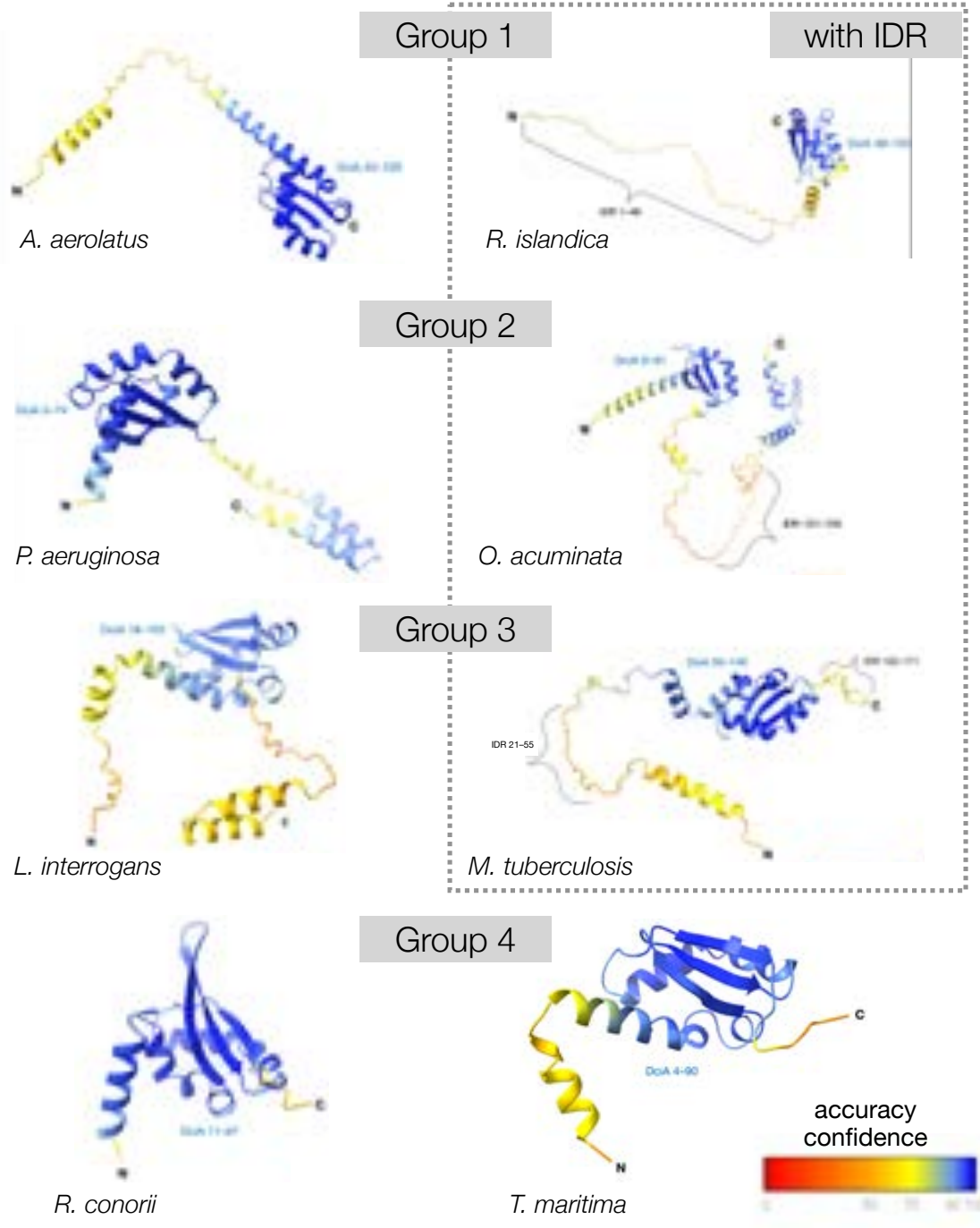
Group 1
with IDR
A. aerolatus
R. islandica
Group 2
P. aeruginosa
O. acuminata
Group 3
L. interrogans
IDR 21–55
M. tuberculosis
Group 4
R. conorii
C
DcA 4-90
N
T. maritima
accuracy
confidence

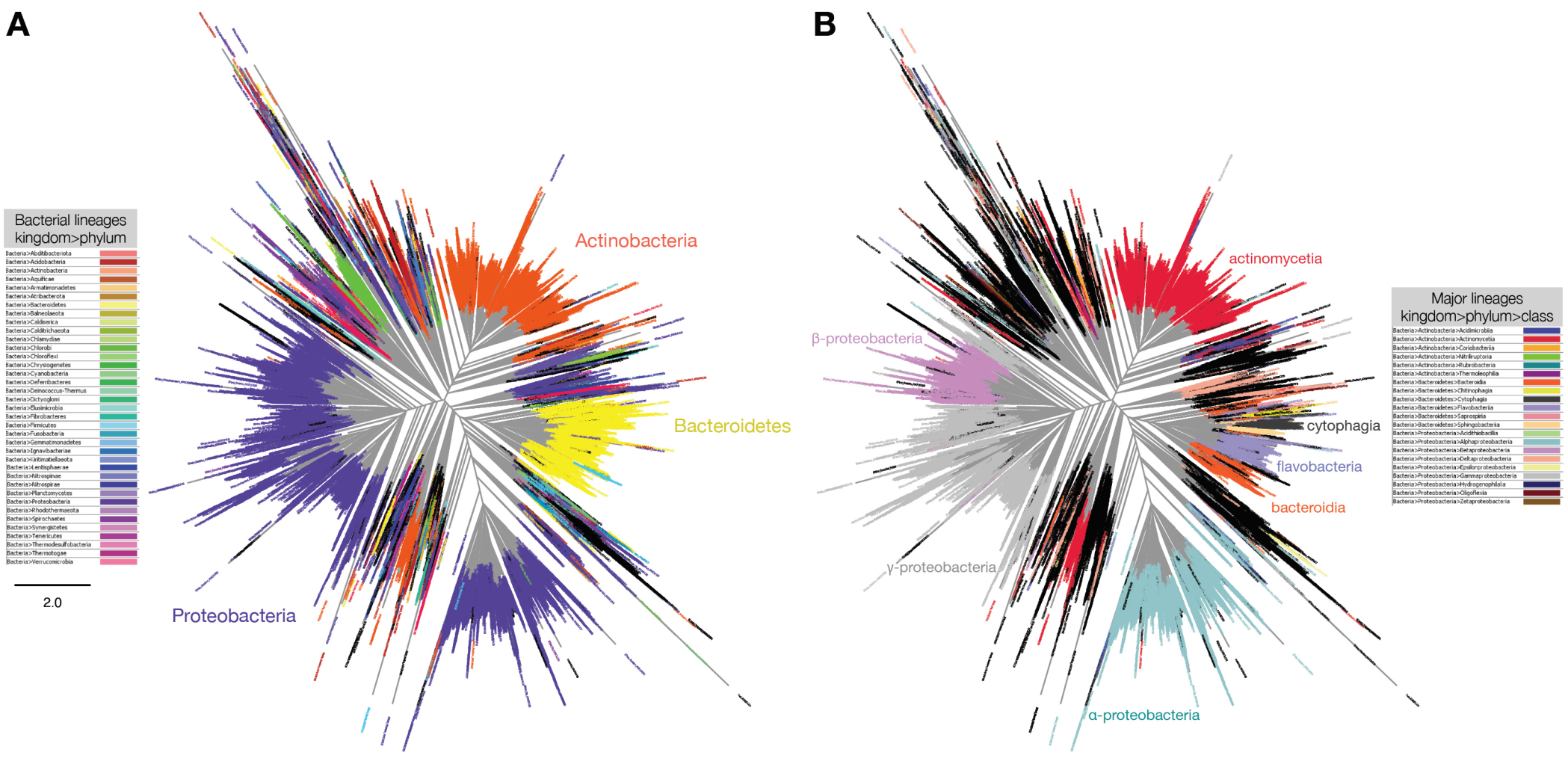
A
Bacterial lineages
kingdom>phylum
Bacteria>Abditibacteriota
Bacteria>Acidobacteria
Bacteria>Actinobacteria
Bacteria>Aquificae
Bacteria>Armatimonadetes
Bacteria>Atribacterota
Bacteria>Bacteroidetes
Bacteria>Balneolaeota
Bacteria>Caldiserica
Bacteria>Calditrichaeota
Bacteria>Chlamydiae
Bacteria>Chlorobi
Bacteria>Chloroflexi
Bacteria>Chrysiogenetes
Bacteria>Cyanobacteria
Bacteria>Deferribacteres
Bacteria>Deinococcus-Thermus
Bacteria>Dictyoglomi
Bacteria>Elusimicrobia
Bacteria>Fibrobacteres
Bacteria>Firmicutes
Bacteria>Fusobacteria
Bacteria>Gemmatimonadetes
Bacteria>Ignavibacteriae
Bacteria>Kiritimatiellaeota
Bacteria>Lentisphaerae
Bacteria>Nitrospinae
Bacteria>Nitrospirae
Bacteria>Planctomycetes
Bacteria>Proteobacteria
Bacteria>Rhodothermaeota
Bacteria>Spirochaetes
Bacteria>Synergistetes
Bacteria>Tenericutes
Bacteria>Thermodesulfobacteria
Bacteria>Thermotogae
Bacteria>Verrucomicrobia
2.0
Actinobacteria
Bacteroidetes
Proteobacteria
B
actinomycetia
β-proteobacteria
cytophagia
flavobacteria
bacteroidia
γ-proteobacteria
α-proteobacteria
Major lineages
kingdom>phylum>class
Bacteria>Actinobacteria>Acidimicrobiia
Bacteria>Actinobacteria>Actinomycetia
Bacteria>Actinobacteria>Coriobacteriia
Bacteria>Actinobacteria>Nitriliruptoria
Bacteria>Actinobacteria>Rubrobacteria
Bacteria>Actinobacteria>Thermoleophilia
Bacteria>Bacteroidetes>Bacteroidia
Bacteria>Bacteroidetes>Chitinophagia
Bacteria>Bacteroidetes>Cytophagia
Bacteria>Bacteroidetes>Flavobacteria
Bacteria>Bacteroidetes>Saprospiria
Bacteria>Bacteroidetes>Sphingobacteriia
Bacteria>Proteobacteria>Acidithiobacillia
Bacteria>Proteobacteria>Alphaproteobacteria
Bacteria>Proteobacteria>Betaproteobacteria
Bacteria>Proteobacteria>Deltaproteobacteria
Bacteria>Proteobacteria>Epsilonproteobacteria
Bacteria>Proteobacteria>Gammaproteobacteria
Bacteria>Proteobacteria>Hydrogenophilalia
Bacteria>Proteobacteria>Oligoflexia
Bacteria>Proteobacteria>Zetaproteobacteria